RESEARCH ARTICLE

VOLCANICA

The influence of vegetation cover on the grain-size distributions and thicknesses of two Icelandic tephra layers

Conner A. G. Morison*[α,β] and Richard T. Streeter[α]

[α] School of Geography and Sustainable Development, University of St Andrews, Irvine Building, North Street, St Andrews, Scotland, UK.
[β] School of GeoSciences, University of Edinburgh, Drummond Street, Edinburgh, Scotland, UK.

Abstract

Grain-size distributions and thicknesses of tephra layers are used to reconstruct characteristics, dynamics, and hazards of explosive volcanic eruptions, but the extent to which the preservation of tephra is influenced by depositional environments is unclear. This paper analyses grain-size distributions and thicknesses of tephra layers produced by the Eyjafjallajökull (2010) and Grímsvötn (2011) eruptions. We collected 110 tephra samples and layer thickness measurements from 86 sites at two locations in southern Iceland. Areas of different vegetation cover have varying capacities to affect rates of tephra erosion, retain fallout, or capture remobilised tephra. The Grímsvötn tephra was somewhat coarser-grained and thicker in areas of birch woodland than in adjacent moss heath, but no comparable differences in the Eyjafjallajökull tephra were observed. The spatial variability (over tens of metres) of median particle-size and layer thickness is low, providing confidence that relatively few samples and measurements may be required to capture fallout characteristics.

Ágrip

Kornastærðargreining á gjósku og gjóskuþykktir hafa verið notaðar í eldfjallafræði til þess að meta ráðandi stærðir og breytur í goshegðun, en þó er lítið vitað um það hvort og hvernig umhverfið hefur áhrif á kornastæðardreifingu og gjóskuþykktum gjóskulaga. Þessi rannsókn snýst um athuganir á kornastærðardreifingu og þykkt gjóskulaganna sem mynduðust í gosunum í Eyjafjöllum (2010) og Grímsvötnum (2011). Við mældum gjóskuþykktir í 86 sniðum og söfnuðum 110 gjóskusýnum á tveimur svæðum á Suðurlandi með ólíkt gróðurfar. Mismunandi gróðurfar hefur áhrif á varðveislu og samþjöppun gjóskufalls, ásamt því að grípa endurflutta gjósku. Grímsvatnagjóskan (2011) var að meðaltali grófari í korninu og þykkari á svæðum þakið birkiskógi en á svæðum einungis með lággróðri, en Eyjafjallagjóskan (2010) sýndi engin slík tengsl. Miðgildið kornastærðardreifinganna og þykktin gjóskulaganna eru ekki mjög mismunandi á þessum sniðum (yfir tugum metra), sem bendir til þess að vísindamenn þurfa tiltölulega litla úrtaksstærð til að fanga breytur í goshegðun.

Keywords: Eyjafjallajökull; Grimsvötn; Volcanic ash; Granulometry; Eruption source parameters; Remobilisation.

1 Introduction

Tephra layers provide insight into the characteristics, dynamics, and hazards associated with explosive volcanic eruptions [Taddeucci et al. 2007]. Their grain-size distributions and thicknesses can be sampled during an eruption to understand how pristine tephra is dispersed through the atmosphere and across terrestrial environments [Bonadonna et al. 2011; Taddeucci et al. 2011; Gudmundsson et al. 2012a; Alfano et al. 2016]. More commonly, the deposits are sampled following weeks to years of surface exposure [Sarna-Wojcicki et al. 1981; Carey and Sigurdsson 1982; Eychenne et al. 2011; Andronico et al. 2014; Bonadonna et al. 2015]. The dynamics of eruptions, their Volcanic Explosivity Index [VEI; Newhall and Self 1982], and eruption source parameters for numerical dispersal modelling (e.g. total grain-size distribution and volume) may be reconstructed from ancient tephra layers produced by eruptions that occurred centuries [Carey et al. 2010; Barsotti et al. 2018; Janebo et al. 2018] to millennia ago [Tsunematsu and Bonadonna 2015; Buckland et al. 2020; Poret et al. 2020]. Yet, it is also known that tephra deposits are modified by syn- and post-depositional processes such as post-eruptive aeolian remobilisation [Blong et al. 2017]. This reworking and modification can continue for years to decades [Wilson et al. 2011; Thorarinsdottir and Arnalds 2012; Arnalds et al. 2013; Liu et al. 2014; Panebianco et al. 2017; Domínguez et al. 2020]. For this reason, grain-size distribution measurements are best taken in real-time [Pioli et al. 2019], although it is more common to sample tephra after the eruption has ended. However, in order to extend the short and patchy record of volcanic eruptions, we are reliant on preserved tephra layers that may have undergone modification during or after their deposition [e.g. Costa et al. 2016; Cashman and Rust 2019]. For these reasons, we require a greater understanding of how representative the characteristics of tephra layers are of initial fallout deposits.

Tephra layers preserved in sedimentary sections are widely used for dating purposes through tephrochronology [Lowe 2011]. However, it is also recognised that tephra layers may be used in applications 'beyond chronology', such as the reconstruction of palaeoenvironmental landforms [Dugmore and Newton 2012; Streeter and Dugmore 2013; Dugmore et al. 2019; Thompson et al. 2021]. The way in which tephra preservation may be affected by the surface environment can also give us an insight into an important phase in the 'life-cycle' of volcanic ash [Ayris and Delmelle 2012; Domínguez et al. 2020; Cutler et al. 2021; Paredes-Mariño et al. 2022]. Recent studies have demonstrated that tephra layer preservation is influenced

* conner.morison@ed.ac.uk

Editor: P. Delmelle | Typesetter: J. Farquharson

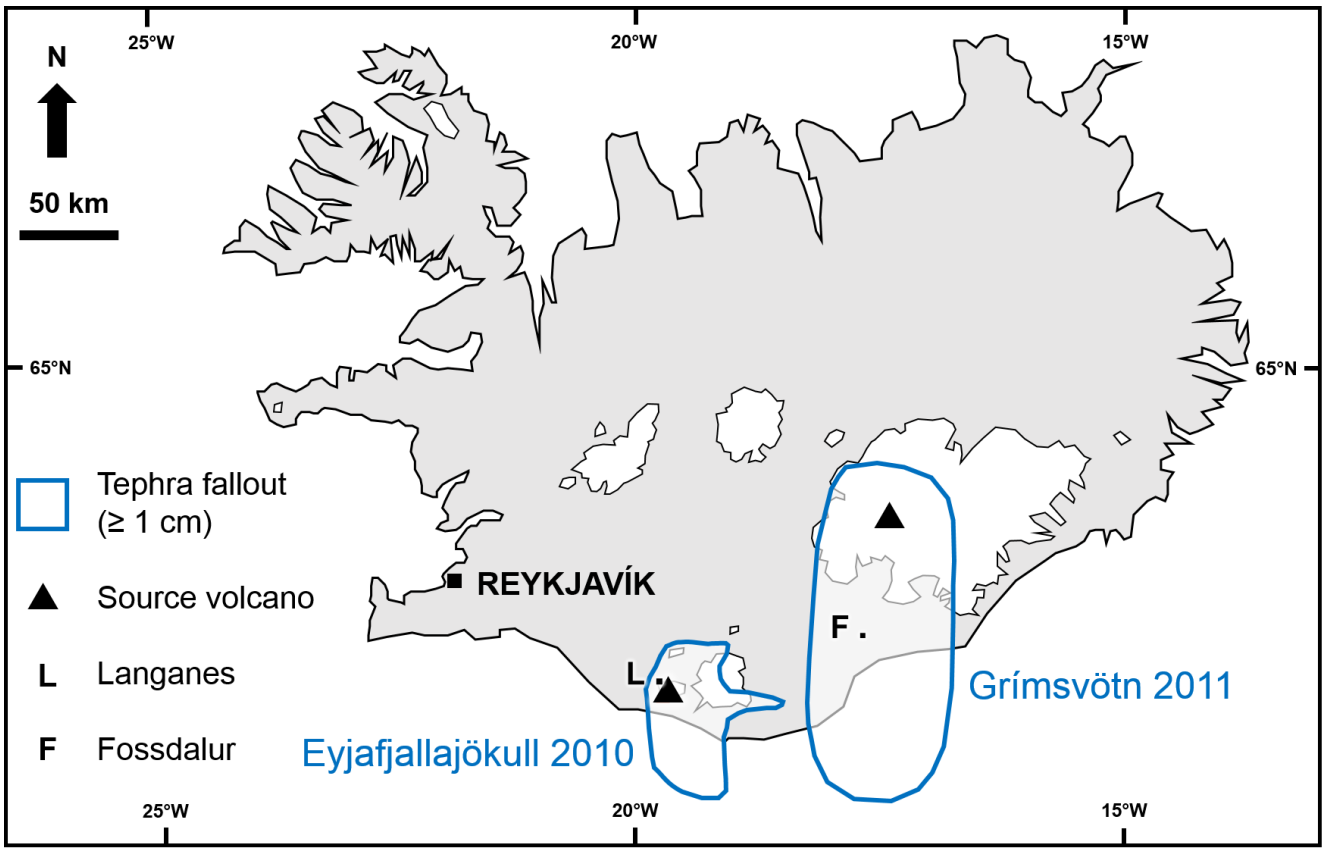

Figure 1: Map of Iceland showing the research locations (Langanes and Fossdalur) and the areas of tephra fallout (Eyjafjallajökull 2010 and Grímsvötn 2011) that exceeded 1 cm in thickness.

by an array of environmental factors—these include vegetation cover, wind patterns, precipitation events, and atmospheric humidity. For example, tephra layer thickness is influenced by surface vegetation cover [Cutler et al. 2016a; b; Dugmore et al. 2018]. Certain fractions of a tephra deposit's grain-size distribution are more liable to syn- and post-depositional remobilisation by the wind [Del Bello et al. 2021]. One recent study in Patagonia was able to infer the post-depositional processes of tephra transport through characterisation of the modified deposits [Domínguez et al. 2020]. That study noted the importance of precipitation events in locking-down deposits and minimising future reworking; we also know that increasing humidity makes it harder for wind to remobilise tephra [Del Bello et al. 2018]. Precipitation regimes are likely to be important for any assessment of the stability of volcanic ash, but there is a lack of consideration of tephra deposit stability in humid and well vegetated environments.

1.1 Aims and hypotheses

This project focussed on testing the reliability of terrestrial tephra layers as archives of the associated Icelandic eruptions of Eyjafjallajökull in 2010 and Grímsvötn in 2011 (Figure 1).

Firstly, we aimed to provide insights into the linkages between vegetation cover and the preserved grain-size distributions and thicknesses of tephra layers. Recent studies have demonstrated links between the structure of vegetation cover (during fallout) and the preserved thickness of tephra layers [Cutler et al. 2016a; b; Dugmore et al. 2018]. To assess whether vegetation cover influences the preserved grain-size distribution of the tephra layers, multiple tephra samples and layer thickness measurements were taken from the same location at multiple sites underneath different types of vegetation cover. We hypothesised that the grain-size distribution of tephra preserved at sites under tall shrubs or in woodland is finer than that of tephra preserved at otherwise comparable sites under dwarf-shrub heath or moss heath.

Secondly, we aimed to improve our understanding of the small-scale spatial variability of preserved tephra layer grain-size distributions and thicknesses in terrestrial settings. The representativeness of any one grain-size distribution measurement of the location's true granulometry is often unclear. If the granulometries and layer thicknesses are highly variable (or patchy) at metre-scales, even in apparently homogeneous environments, then a higher number of replicate samples is required. To address our second aim, we investigated whether granulometry and thickness varied at metre-scales within blocks of homogeneous vegetation cover. Our second hypothesis was that similarity in median particle-sizes and layer thicknesses decreases with distance between deposits at metre-scales.

Thirdly, we aimed to investigate the relationship between the thickness and grain-size distribution of the preserved

tephra layer. The identification of a correlation between tephra layer particle-size and thickness within a small area (in our case, up to 140 m between sites) may help to identify the occurrence of remobilisation and redeposition. On landscape-wide (kilometre) scales, the granulometry and thickness of tephra deposits are likely related to distance from the volcano and size-selective depositional processes. However, at the scale of tens of metres, we reasoned that sample sites where the layer is thinner (than at other sites in the same location) may have a coarser median particle-size due to post-depositional reworking of the fallout deposit and loss of fine particulates. Our third hypothesis was that, at the location-scale, sample sites where the layer is thinner have a coarser median particle-size than sample sites where the layer is thicker.

1.2 Eruptions

The Eyjafjallajökull eruption of 2010 (Ey2010 hereinafter) occurred in four phases. On 14 April (phase I), phreatomagmatic explosions occurred as upwelling magma fragmented vigorously through violent interaction with glacial meltwater. The ≤11 km-high plume in phase I deposited a fine-grained benmoreite tephra (SiO_2: ~60 wt.%) with a powdery, flour-like grain-size to the east and south [Gudmundsson et al. 2012a]. On 18 April, a quieter phase (II) began, which saw the effusion of a 3 km-long lava flow down Gígjökull [Gudmundsson et al. 2012a]. A coarser-grained and darker-coloured (sand-like) ash [Gislason et al. 2011] was deposited initially to the southeast, then progressively northwards and westwards [Gudmundsson et al. 2012a]. The start of a second explosive phase (phase III) on 5 May was accompanied by the generation of a more evolved, trachytic (SiO_2: ~65 wt.%) tephra that was deposited to the southeast (but to the south and west on 12–14 May). Tephra was dispersed in all directions until 18 May when the supply of juvenile magma into the evolved silicic magma gradually reduced (phase IV), and the eruption ceased on 22 May [Gudmundsson et al. 2012a]. The entire episode generated a total bulk tephra volume of ~0.27 km^3 across a generally south-easterly dispersal axis, with ~85 % of tephra production having occurred during phases I and III when the tephra was most fine-grained and the particle morphology was most brittle and angular [Figure 2A; Gislason et al. 2011; Gudmundsson et al. 2012a; Horwell et al. 2013]. During the eruption, tephra particles aggregated as they fell from the ash cloud and disaggregated upon impacting the ground [Taddeucci et al. 2011]. Hence—following surface chipping, fragmentation, and disintegration—the fine ash component in the volcano's proximity became proportionally higher than would have been expected without aggregation [Mueller et al. 2017]. The Ey2010 tephra was collected on sheets over a 150-minute period during phase IV of the eruption [Taddeucci et al. 2011] near to our study location at Langanes. However, our samples incorporate the surviving record of the entire eruption. Based on the isopach map published by Gudmundsson et al. [2012a], the thickness of the tephra deposit at Langanes was ~30 mm.

The Grímsvötn eruption of 2011 (G2011 hereinafter) began on 21 May at the ice-capped summit crater. The interaction between magma and glacial meltwater resulted in a phreatomagmatic eruption with a basaltic to basaltic andesite composition [Óladóttir et al. 2011; Horwell et al. 2013; Olsson et al. 2013; Cabré et al. 2016]. The eruption deposited coarser-grained tephra than that of Ey2010 [Liu et al. 2014; Prata et al. 2017]. Tephra fallout from the ≤20 km-high eruption plume was heaviest in the first two days. The fallout was blown to the south, and gradually reduced in intensity until the eruption ended on 28 May. The eruption was short-lived, generating a total bulk tephra volume of ~0.7 km^3 that was dispersed southwards [Gudmundsson et al. 2012b]. The thickness of the tephra deposit at Fossdalur was not recorded immediately after the eruption (Figure 3A). Cabré et al. [2016] reported fallout deposits of 105 and 355 mm thickness from Skeiðarársandur (<5 km southeast of Fossdalur) on 25 May 2011. In June 2014, Cutler et al. [2016a] recorded a mean layer thickness of ~46 mm, 3 km to the south of Fossdalur. Cutler et al. [2016b] recorded a mean layer thickness of ~44 mm (36 mm in moss heath and 52 mm in birch woodland) at our sites in June 2015.

2 Methods

Iceland is an established setting for tephrostratigraphic research [Thordarson and Larsen 2007; Larsen and Eiríksson 2008; Thordarson and Höskuldsson 2008]. Fieldwork was carried out in September 2019 at two locations (Langanes and Fossdalur) in southern Iceland, whereupon we collected 110 samples of tephra at 86 individual sites (Figures 1, 2 and 3; Table 1).

At Langanes (Figure 2A–C), we collected 48 samples of the Ey2010 tephra layer from 36 individual sites across three contrasting vegetation types and across an area of 0.4 km^2. Vegetation cover was categorised as tall shrub, moss heath, and dwarf-shrub heath (Table 2) following Dugmore et al. [2018]. We assumed that the vegetation composition and structure, observed nine years after the eruption, were similar during the eruption. Regular visits over this period verify no notable change in vegetation cover [Dugmore et al. 2013; Streeter and Dugmore 2013] and we understand from landowners that only light grazing by sheep has occurred since 2010. The presence of shrubs in this area indicates that any grazing pressure is likely to be low. The presence of isolated patches of tall shrubs (*Salix phylicifolia;* patches ~5 m in diameter and 25–140 m apart from each other) in areas of moss heath and dwarf-shrub heath, allowed us to investigate the impact of vegetation on tephra layer preservation (Figure 2B).

At Langanes, Ey2010 was identified as a grey, fine- to coarse-grained tephra layer near the surface (Figure 2C). We established four transects across two areas of contrasting vegetation cover (Supplementary Material 1 Figure S1A; Table 2). All four transects incorporated tall shrub cover. Two transects extended into dwarf-shrub heath and two into moss heath. Sampling intervals varied along the transect (Table 2). At each interval, a shallow pit (5–10 cm deep) was excavated and tephra samples were removed—either sub-samples from the upper and lower halves of the layer (Transects 1 and 2) or samples from the whole layer (Transects 3 and 4). Tephra layer thicknesses (lower contact to upper contact) were measured to the nearest millimetre. It is known that measurement

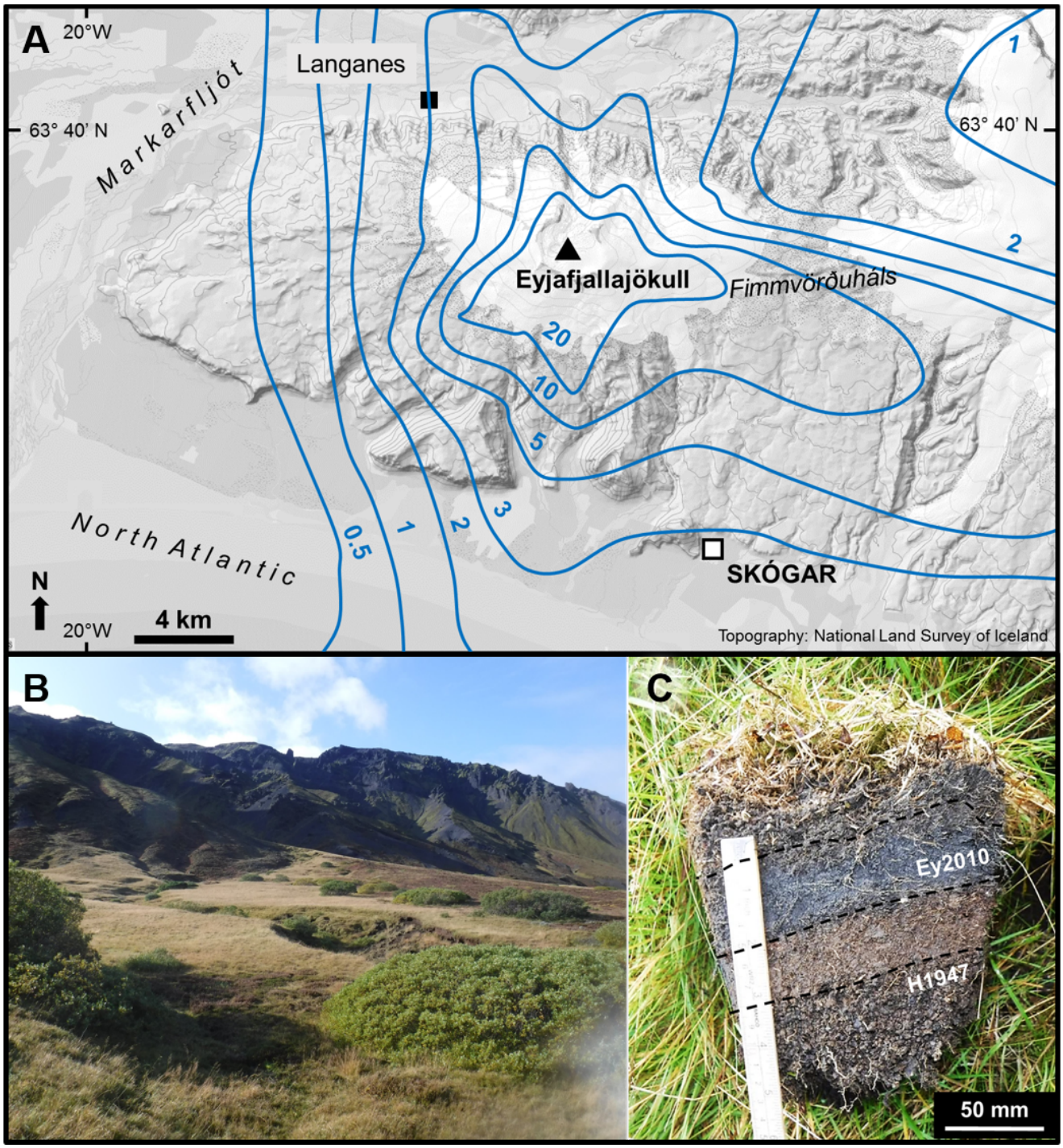

Figure 2: [A] Isopach map of the tephra deposit from the Eyjafjallajökull eruption of 2010 (Ey2010), showing the study location at Langanes. Isolines (cm) are based on Gudmundsson et al. [2012a]. Underlying topography provided by National Land Survey of Iceland [2012]. [B] Overview of the Langanes area showing isolated tall shrubs and the slopes of the volcano in the background. [C] Sample section at Langanes showing tephra from Eyjafjallajökull (2010) near the surface. The tephra layer from the Hekla (1947) eruption was identified at the base of this section, as identified by its stratigraphic context, physical characteristics and section location in relation to the known fallout area [Thorarinsson 1954]. Dashed lines show the indicative contacts between tephra and soil.

Table 1: Number of samples collected at the two locations with additional location information.

Parameter	Location	
	Langanes	Fossdalur
Tephra	Eyjafjallajökull 2010 (Ey2010)	Grímsvötn 2011(G2011)
Date sampled	9 September 2019	6 September 2019
Number of sites sampled	36	50
Number of sub-samples*	24	12
Total number of samples	48	62
Distance from vent (km)	7.3	44.7‡ 45.4¶
Dominant wind direction†	ENE	N§
Precipitation range at nearest weather station† (mm yr^{-1})	2000–2500	1500–2000

* 'Sub-samples' refers to samples of the upper, middle, and lower portions of the tephra layers.
† Data: Veðurstofa Íslands [2012].
‡ Moss heath.
¶ Birch wood.
§ May be influenced by local wind field effect of high topography at Lómagnúpur.

uncertainty can be significant, particularly in the case of thinner tephra layers [Engwell et al. 2013]. At our sites the basal contact was clearly defined by the colour difference from the surrounding soil, and the upper contact was indicated by a marked increase in organic material near the surface. Engwell et al. [2013] noted that measurements are likely to have lower errors where the contacts are clear, therefore we have reasonable confidence that our measurements are accurate. Additional data were recorded using the same methodology at 12 *ad-hoc* sites (six on moss heath, six on dwarf-shrub heath; all within a 140 m radius of the tall shrub patches).

At Fossdalur, we collected 62 samples of the G2011 tephra layer from 50 individual sites across two 0.0001 km^2 areas of contrasting vegetation types. The sampling sites (~45 km south of Grímsvötn, Figure 3B–C) are located on the eastern flanks of Lómagnúpur, near the Núpsvötn glacial meltwater river. Cabré et al. [2016] and Cutler et al. [2016a] noted that this area was probably close to the G2011 plume axis.

We visited the area in the months following the G2011 eruption, so we know that the vegetation cover had not changed notably between our measurements and the period shortly after the eruption. Although the area is not near to a farm and not managed actively for grazing, it is possible that it experiences light sheep grazing during the summer. The two main vegetation cover groups at the study sites were characterised by Cutler et al. [2016b] as homogeneous blocks of downy birch (*Betula pubescens*) woodland and moss heath (dominated by *Racomitrium lanuginosum*). Further details on the vegetation cover are shown in Table 2. The birch woodland sites are <1 km farther from Grímsvötn than the moss heath sites; we assumed that both vegetation cover types received deposits of tephra with similar grain-size distributions and thicknesses [Cutler et al. 2016b].

Two grids were overlain onto the 20 m-long transects used by Cutler et al. [2016b] for sampling in June 2015. Each grid covered an area of 100 m^2 (10 × 10 m) of birch woodland (Figure 3B) and moss heath (Figure 3C) respectively, providing 25 sample sites each, at sampling intervals of 2.5 m. To avoid sampling tephra layers disturbed by the sampling exercise in 2015, each grid was offset from the 2015 transects by 1 m (Supplementary Material 1 Figure S1B).

At Fossdalur, G2011 was easily identifiable as a dark, coarse-grained ash layer near the surface. The tephra deposit has since been incorporated into the stratigraphy at this location (Figure 3D). G2011 was readily distinguished from the surrounding sediment by its colour, grain-size, and by the lack of organic material in the layer in comparison to the surrounding sediments. Although the contacts sometimes appeared diffuse (Figure 3D) it was possible to determine sharp upper and lower contacts reliably upon close observation. At each site, a shallow pit was dug, samples of the G2011 tephra were taken, and layer thickness (lower contact to upper contact) was measured. In both vegetation types, two sub-samples from the lower third, two from the middle third, and two from the upper third of the tephra layer were collected.

2.1 Particle-size analysis

We were guided by the treatment method described by Gee and Bauder [1986]. To dissolve any organic matter in the tephra samples, 10 mL of 30 % hydrogen peroxide (H_2O_2) were added to centrifuge tubes containing each tephra sample and left overnight. The tubes were then placed into a water bath at 80 °C for two hours until the removal of organic matter was complete. For a further two hours, 5 mL of 10 % hydrochloric acid (HCl) were used to dissolve any carbonate material. Whilst HCl was applied in our procedure, we caution against using this agent if the researcher wishes to analyse the tephra composition. Further information on these risks, in particular ferromagnesian cation dissolution in basaltic tephra, can be found in the literature [Gee and Bauder 1980; Blockley et al. 2005; Lowe 2011]. To dilute the samples, 30 mL of deionised water were added to the tubes, which then were

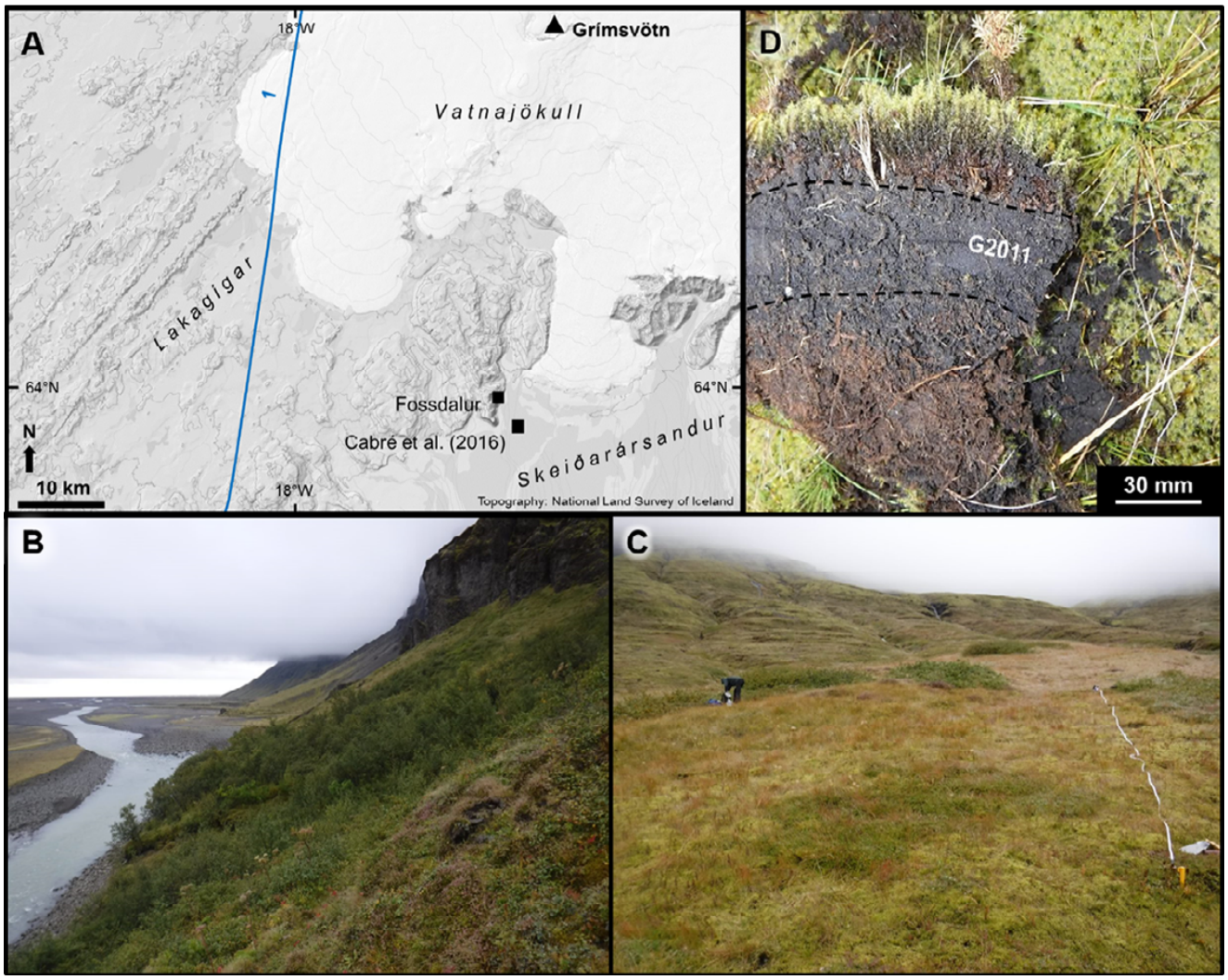

Figure 3: [A] Isopach map of the tephra deposit from the Grímsvötn eruption of 2011 , showing the study location at Fossdalur. The isoline (cm) is based on Thordarson and Höskuldsson [2020]. Topography provided by National Land Survey of Iceland [2012]. [B] The location of the birch woodland sampling grid at Fossdalur, looking south. [C] The location of the moss heath sampling grid at Fossdalur, looking west. [D] Sample section at Fossdalur (moss heath) showing tephra from Grímsvötn (2011) near the surface. Dashed lines show indicative contact between tephra and sediment.

centrifuged at 3000 rpm for five minutes (acceleration 9, brake 6). The less dense supernatant liquid was poured off and the tubes were topped up with deionised water before 5 mL of 5 % sodium hexametaphosphate ($Na_6P_6O_{18}$) were added to ensure that tephra particles did not flocculate in storage.

A Beckman Coulter LS230 Particle-Size Analyser was used to measure the grain-size distribution of the prepared tephra samples, through the detection range of 0.1–2000 µm [Blott et al. 2004] at lens obscuration levels of 8–15 %. The analyser uses an array of photodiode detectors to measure the diffraction of laser beams in channels filled with waterborne tephra particles. We note that, as non-spherical particles are most stable (in motion) when their largest cross-sectional area is perpendicular to the direction of travel, the largest face of the particle will most often be the one that crosses the laser beam. Consequently, the method's main limitation is that the grain-size distribution may be coarse-skewed [Blott et al. 2004; Eshel et al. 2004; Buckland et al. 2021]. The analyser ran each sample thrice, and each distribution is an average of the three grain-size distributions generated for each sample [e.g. Durant et al. 2009; Gatti et al. 2013; Etyemezian et al. 2019].

2.2 Data analysis

Where analysis required data representative of a whole sample, and where we had sub-sampled separately the upper, and lower portions (and in some cases also the middle portion) of the layer, data for a whole sample were generated by using a mean of the upper, middle (if applicable) and lower subsamples (that represent equivalent thicknesses). We describe the grain-size of the tephra layers using the volcaniclastic classification system of White and Houghton [2006], which parallels that of Wentworth [1922]. The logarithmic phi (Φ) scale, where $\Phi = -\log_2(\text{mm})$, is used in analyses of the grain-size distributions of tephra [e.g. Bonadonna and Houghton 2005] where extremes of data differ by several orders of magnitude. The Inman [1952] sorting coefficient (σ_Φ) was calculated using

Table 2: Vegetation cover and sampling site details at Langanes (transects) and Fossdalur (grids; vegetation information from Cutler et al. [2016b]).

Sampling locations	Co-ordinates	Vegetation	
		Start of transect	End of transect
Ey2010			
Transect 1 (LNT1) Altitude: 141 m Length: 10 m Intervals: 2 m Samples: 12	0 m: 63.67815, −19.73311 10 m: 63.67819, −19.73295	Tall shrub: *Salix phylicifolia*	Moss heath: Poaceae, *Equisetum*
Transect 2 (LNT2) Altitude: 145 m Length: 10 m Intervals: 2 m Samples: 12	0 m: 63.67761, −19.73369 10 m: 63.67765, −19.73380	Shrub: *Salix phylicifolia*	Dwarf-shrub heath: *Empetrum nigrum*, *Salix lanata*, *Vaccinium myrtillus*, *Alchemilla alpina*, Poaceae
Transect 3 (LNT3) Altitude: 151 m Length: 7.5 m Intervals: 1.5 m Samples: 6	0 m: 63.67723, −19.73367 7.5 m: 63.67721, −19.73354	Tall shrub: *Salix phylicifolia*	Moss heath: Poaceae, *Equisetum*
Transect 4 (LNT4) Altitude: 151 m Length: 6.25 m Intervals: 1.25 m Samples: 6	0 m: 63.67710, −19.73413 6.25 m: 63.67714, −19.73420	Tall shrub: *Salix phylicifolia*	Dwarf-shrub heath: *Empetrum nigrum*, *Salix herbacea*, *Erica tetralix*, *Alchemilla alpina*, *Salix lanata*, *Vaccinium myrtillus*, Poaceae

Sampling locations	Co-ordinates	Vegetation
G2011		
Moss heath (FDM) Altitude: 160 ±2 m Grid: 10 × 10 m Intervals: 2.5 m	0,0: 63.99857, −17.48278 0,4: 63.99862, −17.48394 4,0: 63.99862, −17.48269 4,4: 63.99871, −17.48284	*Racomitrium lanuginosum* (dominant), *Racomitrium ericoides*, *Sanonia uncinata*, *Kobrobesia myosuroides*, *Trisetum spicatum*, *Thymus praecox*, *Galium verum*, *Bistorta vivipara*, *Equisetum*
Birch woodland (FDB) Altitude: 98 ±2 m Grid: 10 × 10 m Intervals: 2.5 m	0,0: 63.99281, −17.48348 0,4: 63.99282, −17.48353 4,0: 63.99291, −17.48350 4,4: 63.99289, −17.48364	*Betula pubescens* (dominant), *Salix phylicifolia*, *Vaccinium uliginosum*, *Rubus saxatilis*, *Festuca*, *Anthoxanthum odoratum*, *Geranium sylvaticum*, *Angelica sylvestris*, *Hylocomium splendens*

the particle-size found at the 84th and 16th percentiles of each sample, using the equation $\sigma_\Phi = (\Phi_{84} - \Phi_{16})/2$, and described using the interpretation scheme of Blott and Pye [2001]: values found within the ranges 0.70–1.00 are moderately sorted and 1.00–2.00 are poorly sorted. So that the most appropriate tests for statistical difference could be selected for each data subset, we used the Shapiro-Wilk test to ascertain whether parametric or non-parametric tests should be applied to the data. Parametric (normal) distributions of data are indicated by p>0.05 and these p-values are reported in parentheses below.

To test whether the grain-size distribution of tephra preserved at sites under tall shrubs or in woodland is finer than that of tephra preserved at otherwise comparable sites under dwarf-shrub heath or moss heath, we used one-way ANOVA tests. These were run because the following groups of three subsets are normally distributed and we wished to test for significant differences between:

a) Median particle-sizes of Ey2010 tephra in tall shrub (p = 0.41), dwarf-shrub heath (p = 0.66), and moss heath (p = 0.97) at Langanes.

b) Vol.% of Ey2010 tephra in size fractions <6.5 Φ in tall shrub (p = 0.36), dwarf-shrub heath (p = 0.87), and moss heath (p = 0.86) at Langanes.

c) Vol.% of Ey2010 tephra in size fractions >4 Φ in tall shrub (p = 0.90), dwarf-shrub heath (p = 0.62), and moss heath (p = 0.54) at Langanes.

d) Layer thicknesses of Ey2010 tephra in tall shrub (p = 0.11), moss heath (p = 0.90), and dwarf-shrub heath (p = 0.41) at Langanes.

Welch's T-tests were run for the following groups of two subsets because they are normally distributed and we wished to test for significant differences between:

e) Median particle-sizes of G2011 tephra in moss heath (p = 0.38) versus birch woodland (p = 0.38) at Fossdalur.

f) Vol.% of G2011 tephra in size fractions <6.5 Φ in moss heath (p = 0.91) versus birch woodland (p = 0.28) at Fossdalur.

g) Vol.% of G2011 tephra in size fractions >4 Φ in moss heath (p = 0.63) versus birch woodland (p = 0.28) at Fossdalur.

h) Vol.% of Ey2010 tephra in size fractions <6.5 Φ in upper (p = 0.98) versus lower (p = 0.52) portions of the layer at Langanes.

i) Vol.% of Ey2010 tephra in size fractions >4 Φ in upper (p = 0.37) versus lower (p = 0.05) portions of the layer at Langanes.

A Mann-Whitney U-test was run for the following group of two subsets because only one subset is normally distributed and we wished to test for a significant difference between:

j) Layer thicknesses of G2011 tephra in moss heath (p = 0.83) versus birch woodland (p <0.01) at Fossdalur.

To test whether similarity in median particle-sizes and layer thicknesses decreases with increasing distance at metre-scales, variation as a function of position was assessed for spatial autocorrelation. By design, the sample sites are regularly distributed in space. In this case, distance between the sites in each sampling grid is the two-dimensional Euclidean distance. In order to detect any spatial autocorrelation, the R package `ape` [Paradis and Schliep 2019] was used to run global Moran's I-tests on each of the four datasets at Fossdalur. The output values for Moran's I vary from +1 for perfect positive autocorrelation to −1 for perfect negative autocorrelation. The `ncf` package [Bjornstad and Cai 2020] was used to calculate and plot the Moran's I statistic for each lag distance on correlograms in order to demonstrate any relationship between proximity and similarity. To test whether, at the location scale, sample sites where the layers are thinner have coarser median particle-sizes than sites where the layers are thicker, we tested for a significant association between median particle-size and thickness of both tephra layers. A Spearman's Rank correlation coefficient test was chosen because, although the medians were normally distributed at Fossdalur (p = 0.07), they were not normally distributed at Langanes (p <0.01). Thicknesses were not normally distributed at either Langanes (p = 0.03) or Fossdalur (p <0.01).

3 Results

3.1 Grain-size distributions and thicknesses in areas of different vegetation cover

3.1.1 *Ey2010 tephra layer*

Figure 4A shows that the shapes of the grain-size distributions, whether taken from the tall shrub patches, or the surrounding moss heath or dwarf-shrub heath, are unimodal, similarly broad, and positively skewed. Tephra from different vegetation surfaces are unimodal with the same mode (4–5 Φ), although there are slight differences in the distributions (Figure 4B). Moss heath sites have a 2–6 % smaller vol.% at the 3.0–4.5 Φ size fraction, and around a 1 % greater vol.% at the 4.5–8.0 Φ size fraction than the other vegetation cover types.

The grain-size distributions of the Ey2010 tephra layer have similar summary characteristics under different types of vegetation cover (Table 3). The mean of the median particle-sizes for tall shrubs (n = 12) is 4.66 Φ (39.6 ± 12.6 µm), for moss heath (n = 12) is 4.88 Φ (34.0 ± 8.0 µm), and for dwarf-shrub heath (n = 12) is 4.58 Φ (41.9 ± 7.5 µm). There is no significant difference between the median particle-sizes of the three vegetation types (ANOVA: $F_{(2,33)}$ = 2.19, p = 0.13). The proportion of extremely fine (>6.5 Φ, or PM_{10}) and coarse-grained (<4 Φ) ash was similar across different vegetation types (Table 3). Moss heath samples contain slightly higher proportions of the finest particulate (mean: 26.6 ± 5.4 vol.%), whilst samples from the tall shrub (mean: 25.0 ± 6.2 vol.%) and dwarf-shrub heath (mean: 21.8 ± 3.9 vol.%) contain slightly lower proportions. There is no significant difference between the vol.% of PM_{10} in the three vegetation types (ANOVA: $F_{(2,33)}$ = 2.60, p = 0.09). Dwarf-shrub heath samples contained higher proportions of the coarsest material (mean: 33.3 ± 7.4 vol.%), whilst samples from the tall shrub (mean: 30.7 ± 10.7 vol.%) and moss heath (mean: 24.8 ± 8.4 vol.%) contain slightly lower proportions (Table 3). However, there is no significant difference between the vol.% of material >4 Φ in the three vegetation types (ANOVA: $F_{(2,33)}$ = 2.88, p = 0.07). The tephra is similarly poorly sorted in each area (Table 3).

The tephra layer shows within-stratigraphy variation, with slightly finer and more poorly sorted tephra found in the lower units (Figure 4C; Table 3). The shapes of the grain-size distributions, whether taken from the upper or lower portions of the tephra layer, are similarly broad with positive skew (Figure 4D). Both upper and lower units are unimodal with the same mode (4–5 Φ). The mean of the median particle-sizes for the upper sub-sample (n = 12) is 4.41 Φ (47.2 ± 13.9 µm) and for the lower sub-sample (n = 12) is 4.74 Φ (37.4 ± 6.1 µm). Lower sub-samples contain higher proportions of the finest particulate (mean: 26.1 ± 2.8 vol.%) than upper sub-samples (mean: 19.9 ± 4.2 vol.%) (Table 3). The differences in the vol.% of PM_{10} between upper and lower sub-samples are significant (Welch's T-test: $t_{(19.28)}$ = −4.27, p <0.01). Upper sub-samples contain higher proportions of the coarsest material (mean: 36.2 ± 11.1 vol.%), whilst samples from lower sub-samples contain lower proportions (mean: 30.5 ± 5.2 vol.%) (Table 3). However, the differences in the vol.% of material >4 Φ are not significant (Welch's T-test: $t_{(15.59)}$ = 1.59, p = 0.13).

Variations in median particle-size along the transects (Supplementary Material 1 Figure S2A) show that there is no consistent change in median particle-size of tephra from under the tall shrubs (sites A-B-C) versus the surrounding area (sites D-E-F: moss heath along Transects 1 and 3, and dwarf-shrub heath along Transects 2 and 4). Layer thickness does not indicate any significant change in preservation on either side of the shrub edges (Supplementary Material 1 Figure S2B).

At Langanes, we did not find significant differences between the mean thickness of the Ey2010 tephra layer within the willow shrubs (n = 12) and in the surrounding dwarf-shrub heath (n = 12) and moss heath (n = 12) (ANOVA: $F_{(2,33)}$ = 2.57, p = 0.09). However, it is noteworthy that the dwarf-shrub heath sites provided samples that, when averaged, had the coarsest mean and median particle-sizes, and are found in areas where, on average, the layer is thicker (mean: 33.6 ± 5.2 mm) (Table 3).

3.1.2 *G2011 tephra layer*

Figure 5A shows that the shapes of the grain-size distributions taken from birch woodland and moss heath are similarly narrow with weak positive skew. Tephra from different vegetation surfaces are unimodal with the same mode (3 Φ) (Figure 5B).

The grain-size distributions of the G2011 tephra layer, sourced from under different vegetation types, have broadly similar characteristics (Table 3). The mean of the median particle-sizes for birch woodland (n = 25) is 3.09 Φ (117.7 ± 19.3 µm) and for moss heath (n = 25) is 3.26 Φ (104.2 ± 13.0 µm). There was a significant difference between the median particle-sizes of the tephra on birch woodland and moss heath surfaces at Fossdalur (Welch's T-test: $t_{(41.97)}$ = 2.89, p <0.01). Moss heath and birch woodland samples contain near-identical proportions of the finest particulate (means: 4.8 ± 1.1 vol.% and 4.7 ± 1.0 vol.% respectively) (Table 3) and the differences are not significant (Welch's T-test: $t_{(47.96)}$ = 0.37, p = 0.71). Birch woodland samples contain higher proportions of the coarsest (<4 Φ) material (mean: 76.4 ± 5.8 vol.%), whilst samples from moss heath contain lower proportions (mean: 73.1 ± 4.0 vol.%) (Table 3). These differences are significant (Welch's T-test: $t_{(42.37)}$ = −2.33, p = 0.02). The tephra is similarly moderately to poorly sorted in each area (Table 3).

Again, the tephra layer shows within-stratigraphy variation—the layer is finer at the top, but sorting is similar throughout (Figure 5C; Table 3). The shapes of the grain-size distributions, whether taken from the upper or lower portions of the tephra layer, are similarly narrow with weak positive skew (Figure 5D). The portions are unimodal with the same mode (3 Φ). The mean of the median particle-sizes for the upper sub-samples (n = 4) is 3.38 Φ (96.0 ± 11.9 µm) and for the lower sub-samples (n = 4) is 2.82 Φ (141.6 ± 20.1 µm). Upper and lower sub-samples contain similar proportions of the finest particulate (means: 5.2 ± 0.5 vol.% and 6.0 ± 2.2 vol.% respectively) (Table 3). The sample size of the subsets is too low to run statistical tests for difference. Lower sub-samples contain higher proportions of the coarsest material (mean: 78.7 ± 7.2 vol.%), whilst upper sub-samples contain lower proportions of the coarsest material (mean: 70.2 ± 5.5 vol.%) (Table 3).

At Fossdalur, the G2011 tephra layer was significantly thinner in moss heath (mean: 37.2 ± 4.5 mm) than in birch woodland (mean: 48.7 ± 11.2 mm) (Table 3; Mann-Whitney U-test: U = 61.5, p <0.01) and the moss heath area also had significantly finer tephra.

3.2 Small scale particle-size and thickness variability of G2011 tephra layer

Neither any obvious visual clustering of similar values of median particle-sizes or layer thicknesses (within each grid), nor any visual similarity (between grids) were identified. There was no global spatial autocorrelation detected within median particle-sizes in moss heath (Moran's I-test: I = −0.06, p = 0.52) nor birch woodland (Moran's I-test: I<0.01, p = 0.1). Figure 6 shows the Moran's I value for each lag distance in each dataset. No global spatial autocorrelation was detected within tephra layer thicknesses in moss heath (Moran's I-test: I = −0.056, p = 0.623) but it was detected in birch woodland (Moran's I-test: I = 0.044, p <0.001). Overall, this shows that the samples which were more closely positioned to one another were not any more similar in terms of median particle-size or layer thickness than samples at greater distances from one another.

3.3 Association between median particle-size and layer thickness

There was no significant correlation between median particle-size and layer thickness for individual sample sites at either Langanes (Spearman's Rank: ρ_s = 0.24, p = 0.13, Figure 7A) or at Fossdalur (Spearman's Rank: ρ_s = 0.19, p = 0.18, Figure 7B).

4 Discussion

The tephra preserved under areas of taller and denser vegetation cover tended to have a slightly coarser grain-size (i.e. a higher vol.% in the <4 Φ fraction) compared to the same tephra at nearby sites with shorter and more open vegetation cover. We interpret this difference as a more faithful preservation of the primary tephra fallout characteristics in areas of contiguous taller and denser vegetation cover, as opposed to these areas being more effective at capturing remobilised tephra. Within each vegetation cover type, grain-size variability was low between different samples. The relationship between median particle-size and tephra layer thickness for each sample site varied, but in general, areas of vegetation cover which retained thicker deposits tended to have coarser-grained deposits. There is statistically significant evidence for differentiation at Fossdalur, but the evidence at Langanes is more equivocal.

4.1 Vegetation cover and aeolian remobilisation of tephra

Freshly deposited tephra is vulnerable to erosion and remobilisation by the wind. In many landscapes (including Iceland), aeolian remobilisation of fine sediment is significant and can persist for years [e.g. Wilson et al. 2011; Thorarinsdottir and Arnalds 2012; Arnalds et al. 2013; Liu et al. 2014; Forte et al. 2018]. As a result, factors which affect the near-surface wind

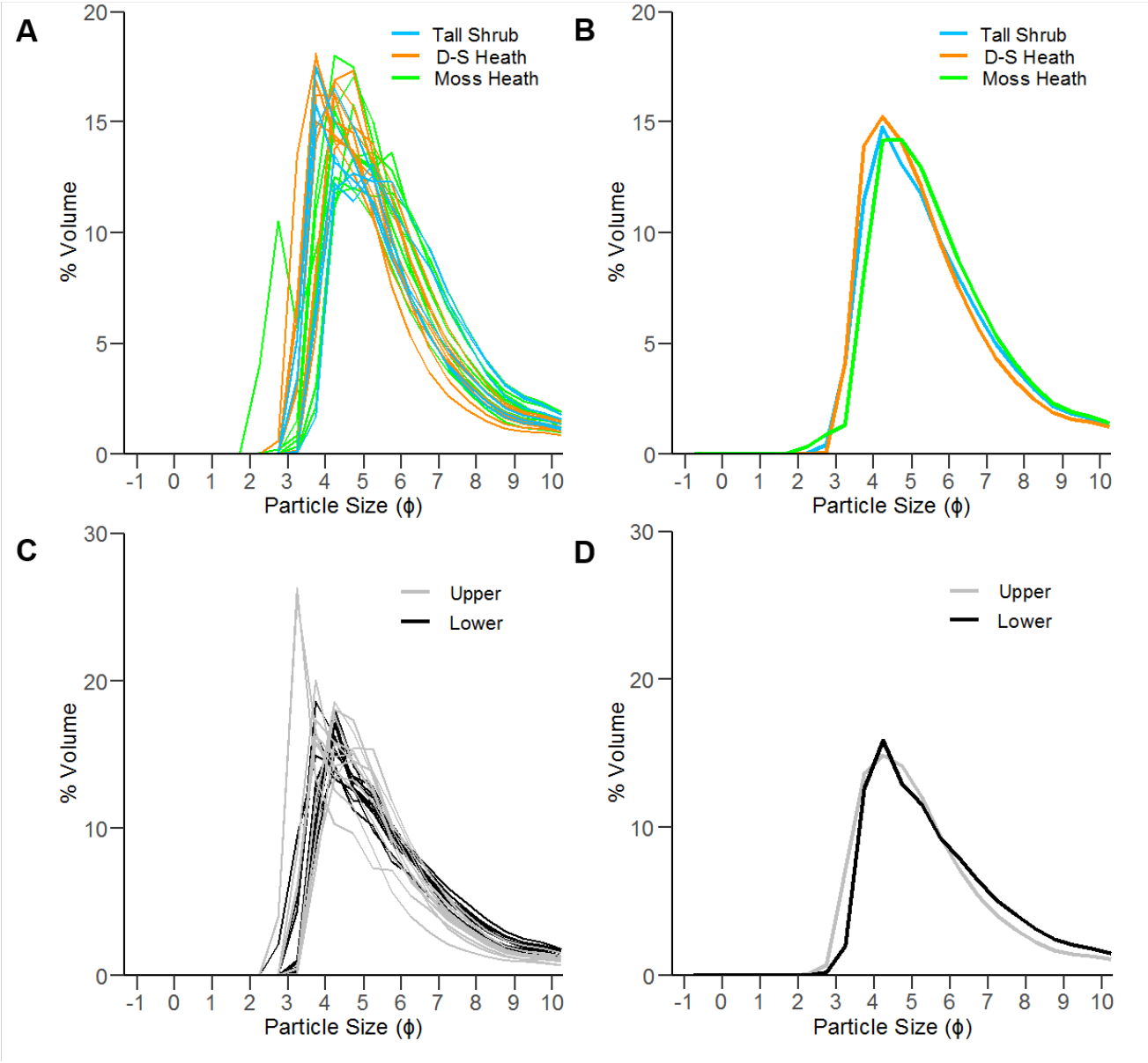

Figure 4: Grain-size distribution plots for samples of Ey2010 taken at Langanes: [A] All samples split by vegetation type (tall shrub = 12, dwarf-shrub (D-S) heath = 12, moss heath = 12), [B] Mean grain-size distributions by vegetation type, [C] Samples taken from different portions of the layer (upper = 12, lower = 12), and [D] Mean grain-size distributions for each sub-sample.

environment (e.g. vegetation cover) are important for determining the degree and extent of tephra remobilisation and reworking [Panebianco et al. 2017; Domínguez et al. 2020]. Here, we discuss how vegetation cover at our Icelandic locations is likely to have influenced the aeolian remobilisation of tephra.

The physical characteristics of vegetation cover (i.e. its height, density, and spatial coverage) play a major role in determining surface roughness, and by extension, the near-surface wind environment. Greater surface roughness reduces surface wind speeds [Gisladottir et al. 2005; Arnalds et al. 2016; Panebianco et al. 2017]. Photogrammetric analyses by Cutler et al. [2016a] revealed a relationship between vegetation structure (height and density) and tephra layer thickness. In the vegetation cover types we studied, there were both short and low-density surfaces (moss heath), medium height but high-density surfaces (dwarf-shrub heath and tall shrubs), and tall but high-density surfaces (birch woodland).

Vegetation may be buried by tephra fallout, potentially affecting the surface wind field by reducing surface roughness. For a period after the eruption, the burial of short stature vegetation may exaggerate differences in the surface wind environment across vegetation cover types. At Langanes and Fossdalur, where initial tephra fallout was 30–50 mm thick, much or all the moss heath vegetation would have been buried. In the birch woodland at Fossdalur, only the understory would have been buried by tephra—and probably only partially, as the understory vegetation was generally taller than the G2011 tephra deposit thickness [Cutler et al. 2016b]. Likewise, the tall and dwarf-shrub vegetation cover at Langanes was taller than Ey2010 tephra deposit thickness. The burial of vegetation at

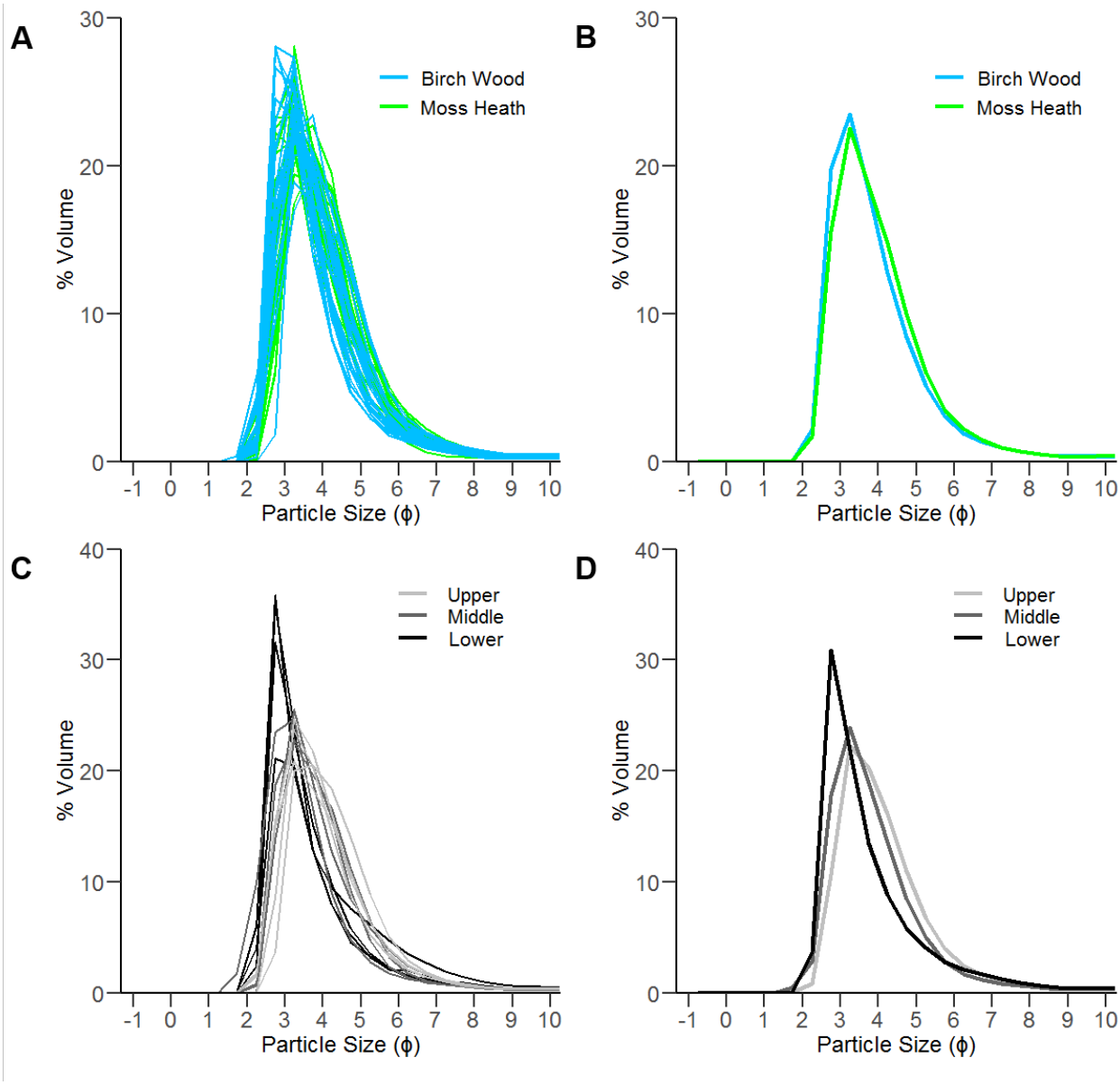

Figure 5: Grain-size distribution plots for samples of G2011 taken at Fossdalur: [A] All samples split by vegetation type (birch woodland = 25, moss heath = 25), [B] Mean grain-size distributions by vegetation type, [C] Samples taken from different portions of the layer (upper = 4, middle = 4, lower = 4), and [D] Mean grain-size distributions for each sub-sample.

locations with moss heath vegetationx probably amplified pre-existing differences in surface roughness between vegetation cover types.

The spatial configuration of vegetation cover at larger scales (tens to hundreds of metres) affects the air flow regime and consequently, the capacity of the air to entrain sediment [Breshears et al. 2009]. Isolated shrubs in areas of lower vegetation cover have a different impact on the wind field than larger contiguous blocks of tall vegetation [Wolfe and Nickling 1993]. Widely spaced low-density shrubs (e.g. Langanes tall shrub patches; Figure 4B) disturb the local wind field. Such obstacles create a wake region where air velocity is reduced on their downwind side [Wolfe and Nickling 1993]. This vegetation configuration can result in identifiable windward and leeward remobilised tephra deposits [Domínguez et al. 2020]. We observed no trend in the properties of the Ey2010 tephra layer outwards from the centres of tall shrubs (Supplementary Material 1 Figure S2A–B). Skimming flow—where the entire surface is within the wake region—predominates once the areal extent of tall vegetation cover is >40 % [Wolfe and Nickling 1993]. The birch woodland at Fossdalur probably experiences such a wind regime.

Collectively, these factors mean that surface wind speeds would have been highest in moss heath areas and lowest in birch woodland and tall shrub areas. Where moss heath and birch woodlands were adjacent and the same tephra was compared (i.e. G2011 sites), the differences in both granulometry and layer thickness were significant. In other respects (e.g. slope and easterly aspect), the sampling sites at Fossdalur were similar, so we suspect that the vegetation cover (in terms of its height, density, spatial configuration, and their effects on

Table 3: Summary of key metrics for the Ey2010 tephra layer at Langanes and the G2011 tephra layer at Fossdalur, split by vegetation cover and portion of layer (± indicates range within 1 standard deviation). Note that vol.% >6.5 Φ is used as a measure of extremely fine ash (PM_{10}) content, whilst vol.% <4 Φ is used as a measure of coarse ash content. According to the interpretation scheme of Blott and Pye [2001], the closer the sorting coefficient (σ_Φ) is to 0, the better sorted the tephra is.

Surface vegetation type	*n*	Mean particle size		Median particle size		Vol.%		Sorting (σ_Φ)	Mean layer thickness (mm)
		(μm)	(Φ)	(μm)	(Φ)	>6.5 Φ	<4 Φ		
Ey2010									
Tall shrub	12	42.3 ± 12.8	4.56	34.0 ± 12.6	4.88	25.0 ± 6.2	30.7 ± 10.7	1.66 ± 0.09	31.0 ± 5.1
Moss heath	12	46.9 ± 12.7	4.41	39.6 ± 8.0	4.66	26.6 ± 5.4	24.8 ± 8.4	1.65 ± 0.14	29.3 ± 3.6
Dwarf-shrub heath	12	49.3 ± 8.1	4.34	41.9 ± 7.5	4.58	21.8 ± 3.9	33.3 ± 7.4	1.60 ± 0.11	33.6 ± 5.2
Upper sub-samples	12	54.1 ± 14.8	4.21	47.0 ± 13.9	4.41	19.9 ± 4.2	36.2 ± 11.1	1.55 ± 0.10	-
Lower sub-samples	12	44.8 ± 6.3	4.48	37.4 ± 6.1	4.74	26.1 ± 2.8	30.5 ± 5.2	1.77 ± 0.06	-
G2011									
Birch wood	25	119.3 ± 14.8	3.07	117.7 ± 19.3	3.09	4.7 ± 1.0	76.4 ± 5.8	0.99 ± 0.08	48.7 ± 11.2
Moss heath	25	109.1 ± 10.6	3.20	104.2 ± 13.0	3.26	4.8 ± 1.1	73.1 ± 4.0	1.04 ± 0.09	37.2 ± 4.5
Upper sub-samples	4	101.0 ± 11.8	3.31	96.0 ± 11.9	3.38	5.2 ± 0.5	70.2 ± 5.5	1.03 ± 0.03	-
Middle sub-samples	4	120.1 ± 20.7	3.06	115.6 ± 20.3	3.11	4.2 ± 1.1	77.5 ± 5.9	0.97 ± 0.09	-
Lower sub-samples	4	134.6 ± 13.4	2.89	141.6 ± 20.1	2.82	6.0 ± 2.2	78.7 ± 7.2	1.09 ± 0.25	-

surface roughness) was the key factor driving their differentiation.

In addition to considering differences in surface wind speed, we consider the susceptibility of different fractions of the grain-size distributions to aeolian entrainment. In order to detach particles from a surface, the wind friction velocity (U^*) must exceed the threshold friction velocity (U^*_{th}) of a particle [Shao and Lu 2000]. Values for U^*_{th} are calculated based on particles' physical properties: particularly their size, density, and shape [Shao and Lu 2000]. The calculated value of U^*_{th} for spherical particles (and ignoring the surface properties) tends to reach its minimum in the 63–125 μm (3–4 Φ) range, and so spherical particles in that size range may be the most susceptible to aeolian remobilisation.

Tephra differs in several crucial respects from other sediments for which values for U^*_{th} are often calculated [Bagheri and Bonadonna 2016]. For instance, tephra is often irregularly shaped and highly vesicular. Therefore, field- and experimental-based approaches have sought to understand how U^*_{th} varies with particle-size for volcanic ash specifically [Del Bello et al. 2018; Etyemezian et al. 2019]. The smallest particles are cohesive (particularly when moist), may form surface crusts, and are more resistant to detachment by the wind [Tarasenko et al. 2019]. The entrainment of larger particles is controlled by their density and requires increasingly high wind velocities [Arnalds et al. 2013]. Recent experimental work, under both laboratory and field conditions, has confirmed that values of U^*_{th} that are based on non-volcanogenic particles tend to overestimate the critical wind speed whilst underestimating the particle-sizes that can be mobilised under expected conditions [Del Bello et al. 2018; Etyemezian et al. 2019]. For two tephra deposits where aeolian remobilisation was measured under field conditions, Del Bello et al. [2021] found that the greatest loss of material occurred in the 100–500 μm (1–3.5 Φ) size range. We suspect that tephra differs from non-volcanogenic material in terms of the maximum size of material that may be remobilised. Collectively, these results suggest that tephra is vulnerable to aeolian remobilisation at somewhat larger size-fractions than many other types of sediment.

Other variables, such as relative humidity and the nature of the substrate, probably affect U^*_{th} for volcanic ash under field conditions [Del Bello et al. 2021]. Experimental results (which also used the Ey2010 tephra) suggest that high humidity tends to increase U^*_{th} for smaller particle-sizes (i.e. <125 μm or >3 Φ), making resuspension more difficult for finer particles in more humid environments [Del Bello et al. 2018; Etyemezian et al. 2019]. However, increased relative humidity made little difference for coarser particles (i.e. 125–250 μm or 2–3 Φ) in these experiments. Another effect observed for the same tephra is a progressive increase in U^*_{th} through time. This was attributed to the removal of the most vulnerable material in earlier runs [Etyemezian et al. 2019; Del Bello et al. 2021].

Field observations in Iceland support the notion that relatively coarse tephra particles are vulnerable to aeolian remobilisation [Arnalds et al. 2013]. These observations demonstrated that very large quantities of ash could be moved from sparsely vegetated surfaces in short time periods (hours) during ash storms (Icelandic: *öskubýlar*) which can reduce visibility to <50 m. During a particularly severe storm, the remobilised Ey2010 tephra included a large proportion of relatively coarse particles: 76 % of particles travelling at 1.2 m in height were in the 0–2 Φ size range [Arnalds et al. 2013]. In such storms, finer particles (32–63 μm or 4–5 Φ) are also remobilised extensively. Liu et al. [2014] reported that tephra from both the Ey2010 and G2011 eruptions reached Reykjavík in an ashy snowstorm in March 2013. Notably, they also observed some coarser particles, suggesting that particles >70 μm (~4 Φ)

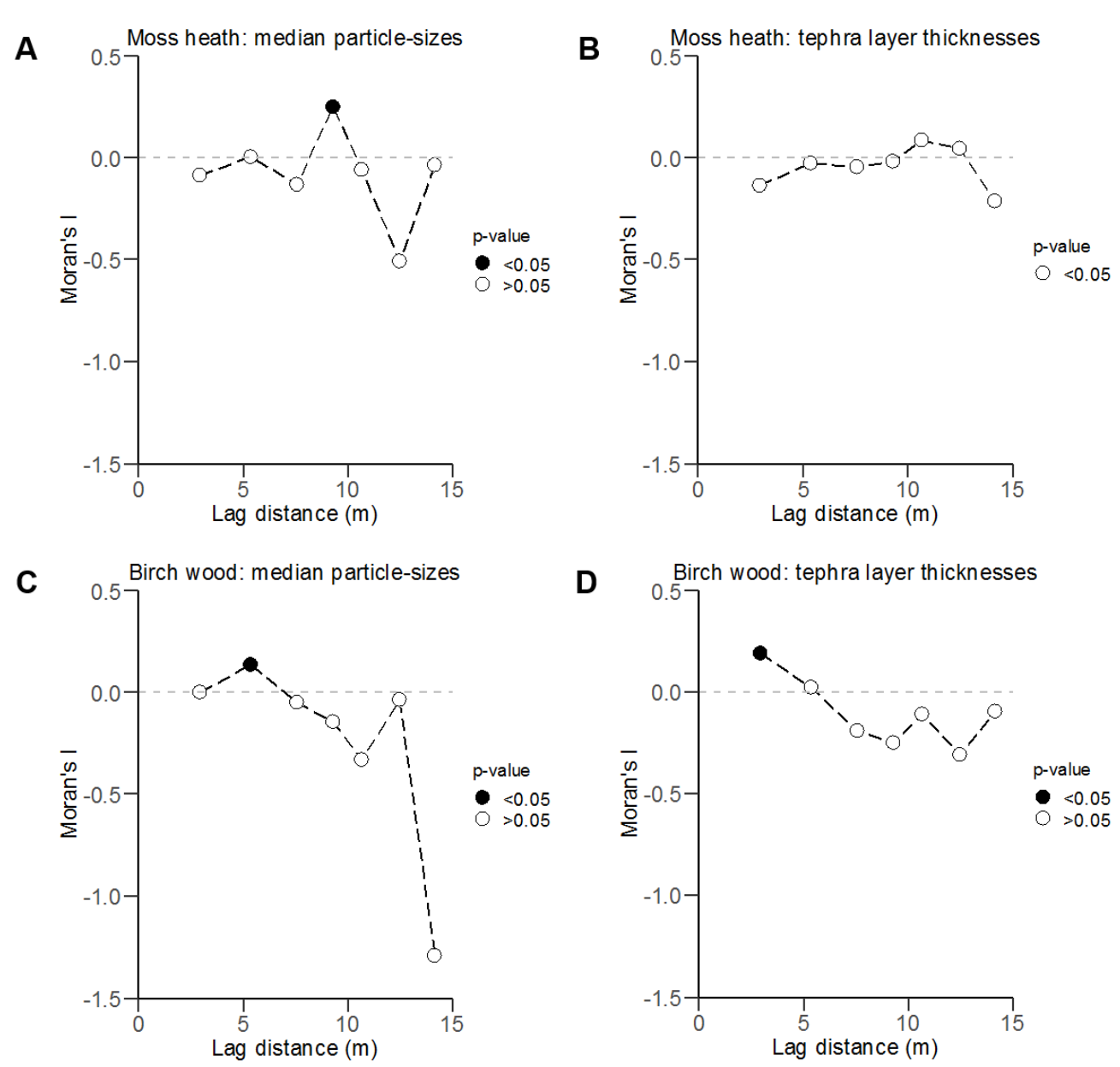

Figure 6: Correlograms showing the Moran's I value and p-values at different distance separations for measurements of the G2011 tephra at Fossdalur. [A] Median particle-sizes in moss heath, [B] layer thicknesses in moss heath, [C] median particle-sizes in birch woodland, and [D] layer thicknesses in birch woodland. Black points indicate significant spatial autocorrelation (p <0.05).

can remain in suspension in some circumstances. Beckett et al. [2017] estimated that ~0.2 Tg of unconsolidated tephra were remobilised during another ash storm in September 2013.

Based on the variation of U^*_{th} with particle-size for comparable tephra deposits, we suspect that the coarser fractions of our tephra samples (approximately 1–4.5 Φ) are readily susceptible to aeolian remobilisation, and may be remobilised in larger volumes than the finer fractions (>4.5 Φ). The proportion of our Ey2010 tephra samples which was <4 Φ was 29 ± 9 vol.%, compared to 74 ± 5 vol.% for our G2011 tephra samples. This difference between the two tephra layers' size fractions that are potentially most vulnerable to remobilisation may explain why we observed greater changes (in granulometry and layer thickness) at Fossdalur than at Langanes (Ey2010). Overall, we hypothesise that, due to their generally lower surface wind speeds, areas of taller vegetation are more likely to retain tephra fallout deposits, particularly in size fractions that are vulnerable to remobilisation.

4.2 Small-scale granulometric variability of tephra layers

Tephra can provide a 'comprehensive record of volcanism' [Lowe and Hunt 2001] but rarely are multiple grain-size distribution measurements collected in one location. Therefore, it is often unclear how representative of the true granulometry any one measurement of grain-size distribution is. For

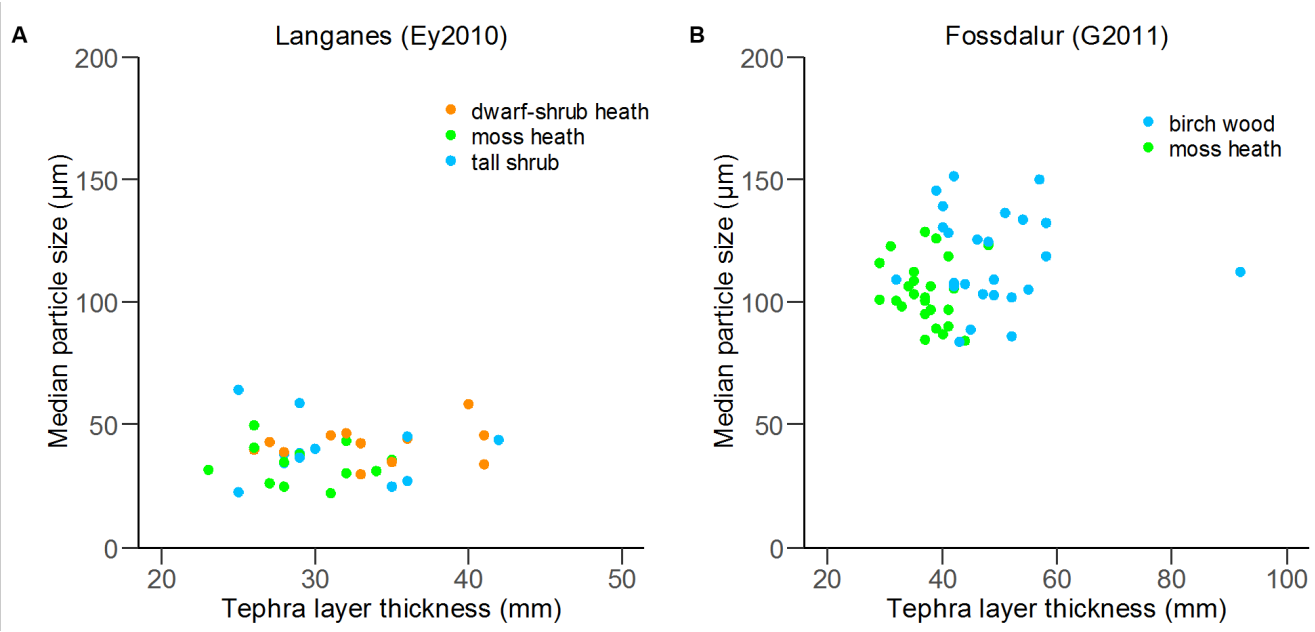

Figure 7: Association between median particle-size and tephra layer thickness at [A] Langanes (Ey2010, $n = 36$) and [B] Fossdalur (G2011, $n = 50$).

example, the grain-size distributions of G2011 samples collected from Skeiðarársandur by Cabré et al. [2016] are highly variable (Figure 8). If the grain-size distribution does not vary markedly, fewer measurements will be needed to capture a good approximation of the true granulometry. However, if granulometry is highly variable at small scales (of up to tens of metres), more effort should be made to collect replicate samples.

At both of our locations, the degree of variability and the differences in the shapes of the grain-size distributions were small (Figures 2 and 3). Almost all sites had broadly similar grain-size distributions. For instance, all the G2011 samples' grain-size distributions were unimodal, with a steep increase in vol.% between 2 and 4 Φ, then a more gradual decrease in vol.% between 4 and 10 Φ. This suggests that, although the sampling sites at our locations were probably subtly different in a range of ways which might be expected to affect the preservation of tephra (e.g. microtopography and proximity to areas of tephra reworking), these variations were relatively unimportant. Instead, the macro-scale features of these grain-size distributions can be captured from relatively few measurements.

We anticipated that, if granulometry was affected by subtle changes in surface conditions and vegetation cover, and if these variations were patchy, then the tephra might also exhibit spatial patchiness, having clusters of coarser- or finer-grained material. The weak global spatial autocorrelation which was detected in the layer thicknesses in the birch woodland is probably only significant because Moran's I-tests are sensitive to outliers, and one site had a layer twice as thick as the mean thickness. Otherwise, we did not detect any consistent pattern of spatial autocorrelation in the grain-sizes and thicknesses of our tephra samples (Figure 6). However, our sampling resolution (metre-scale) may be too coarse to capture the optimal scales of spatial autocorrelation in our chosen metrics. There is no evidence for spatial structure in terms of grain-size and thickness variation. A similar study found autocorrelation in tephra layer thickness only at short (~3 m) separations [Cutler et al. 2016b]. Engwell et al. [2013] found that variability in thickness measurements increased from low levels of variability at 0.1 m separation to higher levels at 1 and 10 m spacing. Higher variability suggests measurements which are not as well spatially correlated, supporting the idea that our sampling resolution was probably too coarse to detect any spatial autocorrelation. Furthermore, our sample size was relatively small so only large effects were likely to be detected.

The relative grain-size homogeneity contrasts with the particle-size measurements of tephra from the eruption of Puyehue-Cordón Caulle in 2011 (CC2011). Domínguez et al. [2020] showed considerable granulometric differences at fine scales between different sampling environments, such as on windward and leeward sides of plants. Both Iceland and Patagonia are windy regions and have experienced extensive soil erosion and ash remobilisation events after recent eruptions [Thorsteinsson et al. 2012; Forte et al. 2018]. A notable difference between those environments is their annual precipitation. Our Icelandic locations receive 1500–2500 mm yr^{-1} precipitation, compared to the Patagonian locations described by Domínguez et al. [2020] that receive <500 mm yr^{-1}. This probably affects preservation in two ways. Firstly, individual precipitation events, if large enough, can greatly reduce ash remobilisation [e.g. Forte et al. 2018]. In the three months after the Ey2010 and G2011 eruptions, 213 mm (Sámsstaðir; June–August 2010) and 318 mm (Kirkjubæjarklaustur; June–August 2011) of precipitation occurred at the nearest weather stations to our sample sites [Veðurstofa Íslands 2012]. In comparison, <30 mm (Ingeniero Jacobacci; June–August 2011) fell in the first three months after the onset of the CC2011 eruption [Fig-

ure 4B in Domínguez et al. 2020]. Secondly, vegetation cover is extensive at our Icelandic locations, compared to the sparse vegetation cover in Patagonia described by Domínguez et al. [2020]. In Iceland, Dugmore et al. [2018] noted that moderate slopes, where vegetation cover was complete, were able to stabilise tephra deposits <10 cm thick. Together, these factors may explain the relative uniformity in grain-size at our locations, when compared to the variability observed elsewhere.

4.3 Interpretation of differences across vegetation cover types

Differences in preserved tephra deposits might arise due to differences in the ability of surfaces to retain or capture material in both the syn-depositional and post-depositional phases [Dugmore et al. 2018]. Within our Icelandic tephra deposits, we observed differences in the preserved thickness of tephra, as well as the preserved grain-size distributions of the tephra. Generally thicker and coarser deposits were found in areas of taller vegetation—we consider two possible explanations for this. Firstly, areas with taller vegetation cover may have retained a greater proportion of the primary fallout deposit. Secondly, areas with taller vegetation cover may have retained primary fallout deposits, but which are overlain or intermixed with accumulated remobilised tephra (secondary deposits). The most likely scenario may be difficult to determine because the factors which are likely to promote retention of the primary deposit are the same factors which are likely to promote the capture of remobilised tephra.

4.3.1 *Eyjafjallajökull tephra*

In or around Icelandic shrub or woodland areas, tephra layers tend to be thicker than those in surrounding areas [Thorarinsson 1958; Cutler et al. 2016a; Dugmore et al. 2018]. Dugmore et al. [2018] argued that the preserved Ey2010 tephra layer, found in tall shrubs at Langanes, was thicker than the nearest (interpolated) thickness measurement from shortly after the eruption. They speculated that the most likely explanation was greater capture of remobilised secondary material during the post-depositional phase, in a similar way that isolated shrubs do for snow thicknesses [Hiemstra et al. 2002; 2006; Essery and Pomeroy 2004]. We observed ash storms and mists (Icelandic: *öskumistur*) at Langanes during the months and years after the eruption, so we know that aeolian remobilisation of tephra has occurred there. Tephra deposits at Langanes had a sharp upper contact with overlying non-volcanogenic sediment, even when observed in the first couple of years after the eruption [Streeter and Dugmore 2013]. This suggests that any alterations to the tephra deposit were limited to the initial months to years after the eruption. Our thickness data (based on a smaller dataset) do not show significantly different thicknesses in different vegetation types. The granulometric data are also equivocal because grain-size distributions are similar across the three vegetation categories. We do not observe a significant association between median particle-sizes and layer thicknesses (Figure 7A). We are still unable to determine the extent to which the tephra layers in this area were modified between fallout and preservation within the stratigraphy. We had hoped to gain insight into the transformative processes by comparing our data with the data collected during the eruption by Taddeucci et al. [2011]. However, their data were collected on sheets over only 150 minutes of the waning phase (Phase IV) of the eruption, and would not record the entire eruptive episode that tephra layers can potentially represent. However, the broad comparability of our own (and other) layer thickness measurements with nearby measurements at the time [Gudmundsson et al. 2012a; Dugmore et al. 2018] suggests that any addition or loss of material was minimal.

We did find that the Ey2010 tephra layer contains significantly higher proportions of the finest tephra near the base than near the top. Whilst an explanation is outside the scope of this paper, we suggest tentatively that the fine particles have percolated downwards into the interstices between coarser ones, armouring the upper portion over time. This would also explain why the upper sub-samples are better sorted (Table 3). Janebo et al. [2018] suggested that this phenomenon occurred in deposits produced by historical Hekla eruptions. It is unlikely that this is related to the different phases of the eruption because Langanes did not receive any fallout from the ESE-trending plume during Phase I of the eruption [14–18 April; Gudmundsson et al. 2012a].

4.3.2 *Grímsvötn tephra*

At Fossdalur, we observed consistent, if small, differences in granulometry and layer thickness. Our data (and data previously collected at Fossdalur by Cutler et al. [2016b]) show that layer thicknesses are greater in the birch woodland than in moss heath. We show that the (mean) median particle-size was coarsest in birch woodland where the (mean) layer thickness was also greatest (Table 3) but that there is no significant association between median particle-size and layer thickness (Figure 7B). This difference is explained most readily by better retention of the primary deposit in birch woodland areas. We consider comparisons with original fallout and grain-size changes through the layer's stratigraphy.

Our grain-size distributions broadly resemble data (Figure 8) collected from a location <5 km farther south by Cabré et al. [2016]. They collected four samples from two sites in a sparsely vegetated area on Skeiðarársandur (their samples ISG5, ISG6, ISG7, and ISG8). We have combined those grain-size distributions by merging ISG5 and ISG6 into a single distribution, and ISG7 and ISG8 likewise, weighting the individual distributions by the proportion of the layer's thickness they represent (Figure 8). They recorded deposit thicknesses which were considerably thicker than our observations. This may reflect the fact that their thicknesses were measured on 25 May 2011, shortly after the eruption, and possibly prior to any compaction. In addition, this area is more exposed to aeolian remobilisation processes and lacks any vegetation cover to stabilise deposits; it is possible these deposits may have been remobilised prior to measurement (i.e. during the eruption). Whilst the granulometry of our birch woodland and moss heath samples are overall similar (with a unimodal distribution and the same mode) to those sampled by Cabré et al. [2016], there are some differences. Our distributions lack the coarser fraction (0–2 Φ) observed by Cabré et al. [2016] and have a greater proportion of the finer material. Cabré et al.

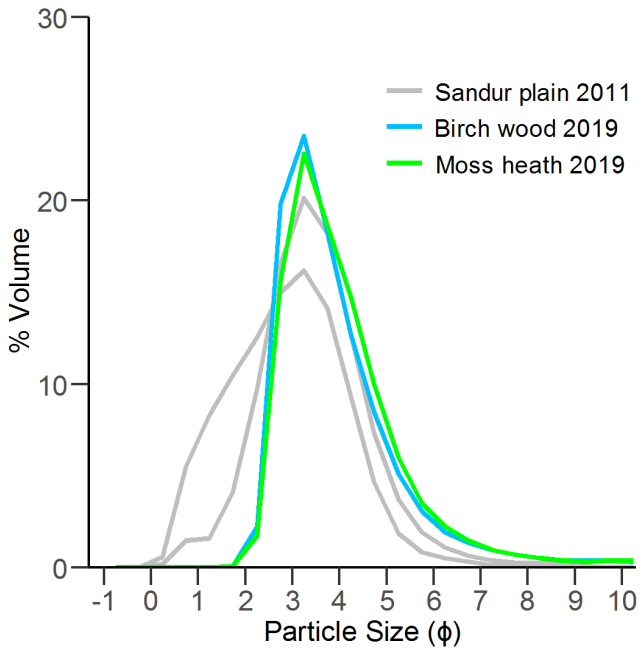

Figure 8: Two weighted grain-size distributions generated from four samples of G2011 tephra taken from Skeiðarársandur on 25 May 2011 by Cabré et al. [2016] (location: 63° 57′ 23″ N 17° 26′ 58″ W) alongside the mean distributions for our samples taken from Fossdalur in September 2019 (moss heath = 25, birch wood = 25).

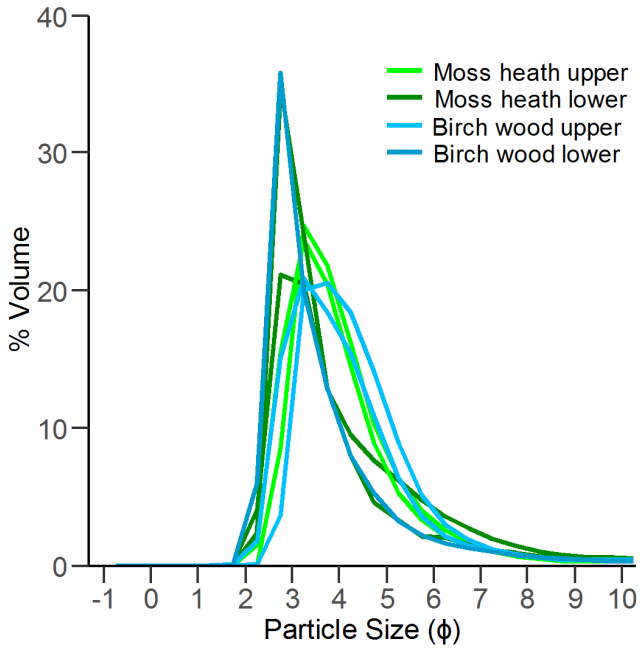

Figure 9: Grain-size distribution plot for samples of G2011 taken at Fossdalur, showing samples taken from different vegetation types and portions (moss heath: upper = 2, lower = 2; birch wood: upper = 2, lower = 2).

[2016] presented the data disaggregated to show the grain-size distributions for the upper and lower portions that they had observed *in situ*. The grain-size distributions of their lower portions closely resembles that of our samples, but their upper portions were coarser-grained. Overall (with the caveats noted above about the differences in the sampling rationale and location), the birch woodland grain-size distributions and thicknesses are closer to that of the fallout samples collected by Cabré et al. [2016] than our moss heath samples. This supports the idea that the greater thickness in birch woodland is due to better retention of primary fallout material there. Should the greater thickness in the birch woodland be due to secondary deposition from size-selective aeolian remobilisation processes, we would expect the grain-size of the tephra in the birch woodland to differ notably from those in the moss heath (which in turn would resemble more closely the original fallout deposit).

Where we have measurements of the lower (n = 4), middle (n = 4), and upper (n = 4) portions of the G2011 layer, there is a consistent reduction in median particle-size from the base to the top of the layer (Figure 5C–D; Table 3). If the birch woodland deposits had been thickened by more effective capture of remobilised ash than the moss heath sites, we would expect the upper sub-samples at the birch woodland sites to be enhanced in the particle-size fractions most susceptible to remobilisation and local transport (0–4 Φ), relative to the moss heath sites where the deposits were thinner. This is not the case—at both the moss heath and birch woodland sites, we observed a similar grain-size distribution in the layer's upper sub-samples (Figure 9). Furthermore, as the tephra at the moss heath sites are overall finer-grained, it would also require the moss heath to be better at capturing remobilised fine ash than the birch woodland. This seems unlikely given the low height and density of the vegetation cover there. Overall, this evaluation suggests that significant volumes of remobilised material did not accumulate at our sampling sites and that they consist of mainly or wholly primary fallout deposits, more of which were retained within the birch woodland.

4.4 Implications for field volcanology

Research using tephra layers to understand the characteristics, dynamics, and hazard of explosive volcanic eruptions requires a better understanding of the extent to which single tephra samples are representative of the tephra layer in that location. For example, the reconstruction of eruption source parameters such as a deposit's volume and Total Grain-Size Distribution relies upon consistent thickness and granulometric characteristics in one location. Several authors [e.g. Dugmore et al. 2019; Sohn and Sohn 2019] have advised that the extent of post-depositional modification of tephra should be assessed. However, relatively few studies have considered in detail the likely extent of post-depositional modification [e.g. Buckland et al. 2020; Cutler et al. 2021].

For the eruptions discussed in this paper, there was a period of months to a few years of extensive aeolian remobilisation events. It is in this early period that tephra deposit properties are most vulnerable to change [Cutler et al. 2021]. The length of this period is likely affected by both the rate of sediment accumulation, and the response of pre-existing vegetation cover to burial. Iceland has some of the highest rates of aeolian remobilisation on Earth [Arnalds et al. 2016], and so

the window for possible surface alteration, even if significant, is probably quite short before burial by windblown material and organic matter. Relatively quickly, soil would have accumulated above the tephra, thereby locking the deposit into the stratigraphy as a layer, and decoupling the tephra from surface processes of transformation [Figure 2C, 3D; Dugmore et al. 2019; Cutler et al. 2021]. In addition, vegetation can often recover quickly following tephra falls of modest thickness by growing through the tephra deposit [e.g. Hotes et al. 2004], inhibiting further transformation of the tephra. The short-stature vegetation found at our study sites would have grown through the tephra, probably in under a year. Previous work on the G2011 tephra observed more or less full vegetation recovery by June 2012 [Streeter and Dugmore 2013]. The taller vegetation was not covered fully in the first place, and the shrubs and trees pre-date the eruptions at both locations [Cutler et al. 2016b; Dugmore et al. 2018]. Therefore, aeolian remobilisation events probably had a lesser effect in areas of contiguous woodland, but more exposed areas like heathlands were likely impacted to a greater extent.

Our analysis shows that post-depositional modification of seemingly primary deposits can alter their attributes but, in the Icelandic locations that we studied, not in a way that is significant for reconstructing the key characteristics of these eruptions. All deposits are contaminated by a degree of 'inheritance' [*sensu* Hall and Thorn 2011]: the temporal contamination of the tephra set by its own characteristics (e.g. chemical composition and granulometry) after deposition. All sampling sites are contaminated by a degree of 'interference' [*sensu* Hall and Thorn 2011]: the spatial contamination of the tephra caused by landscape heterogeneity (e.g. woodlands, glaciers, lakes, *sandur* plains) in the fallout zone. For the purposes of sampling the least contaminated tephra, certain sampling sites are preferable over others.

The preservation environment is important, particularly where eruptions deposit material over a wide range of environments [e.g. Buckland et al. 2020]. In Iceland, our research suggests that contiguous woodlands, present at the time of the eruption, could be the best locations from which to source the least altered tephra fallout. Prior to the settlement of Iceland (Icelandic: *Landnám*) in the ninth century CE, birch woodlands occupied much of the lowlands, where the climate was favourable and the land surface was stable. However, Iceland lost most of its woodland cover during the centuries after settlement [Dugmore et al. 2000; Streeter et al. 2015]. This limits the opportunities to sample historical tephra layers that have experienced the least 'interference' during their transformation into the stratigraphy. In the future, afforested areas, such as Hekluskógar (a 900 km^2 woodland area planted in 2005), will increase the landscape's capacity to lock-down tephra as it falls [Ágústsdóttir 2015], limiting subsequent remobilisation and alteration of tephra deposits in these areas. Our findings also suggest that grain-size distributions and thicknesses of tephra fallout deposits would be faithfully preserved in volcanic regions where forests have existed for millennia (e.g. the Cascades Volcanic Arc). For instance, the temperate rainforests of North America's Pacific seaboard received and preserved representative fallout thickness and grain-size distributions from the eruption of Mount St. Helens in 1980 [Cutler et al. 2018; 2020; 2021]. This should give confidence to volcanologists who sample tephra layers from historical and prehistorical eruptions in regions where extensive forests have been long established.

5 Conclusions

We tested three hypotheses about how tephra layer characteristics vary across different environments. Our study suggests that, in the case of the G2011 tephra, notable granulometric differences within and across a tephra layer may be created by differences in vegetation cover. However, these differences were not observed for the Ey2010 tephra. For G2011, and in contrast to our expectations, taller vegetation tended to retain slightly coarser-grained tephra. This likely reflects the sensitivity of even relatively coarse tephra particles to aeolian remobilisation. Where vegetation cover is complete and tephra fallout thickness is modest (<10 cm), the spatial variability (over tens of metres) of the layer's granulometry is low. This provides confidence that relatively few samples and measurements may be required to accurately capture key tephra characteristics. In general, locations with a thinner (mean) tephra thickness had a finer (mean) median particle-size, although there was no significant association between median particle-size and layer thickness. This information has given us a better understanding of the history of tephra transformation at Langanes and Fossdalur. Therefore, we suggest that, of the original volume of material deposited in birch woodlands, little was remobilised by the wind. Consequently, birch woodlands which were present at the time of the eruption could be the best locations in Iceland from which to source archived tephra fallout.

Author Contributions

CAGM and RTS contributed to the conceptualisation, methodology, analysis, visualisations, and writing of this paper.

Acknowledgements

Many colleagues influenced the thesis [Morison 2020] from which this paper is drawn. We thank Willem Koster for assisting in data collection and Will Hiles (both of University of St Andrews) for providing training and assistance when undertaking particle-size analysis. Discussion with Polly Thompson (University of Edinburgh) was helpful for navigating some of the technicalities of tephra preparation and analysis. Ian Lawson (University of St Andrews) and Nick Cutler (Newcastle University) provided helpful comments on early drafts. Jose-Luis Fernandez-Turiel (Geociencias Barcelona) kindly provided data collected on Skeiðarársandur in 2011 (Figure 8). We are grateful to Þorvaldur Þórðarson (University of Iceland) and Max Naylor for proof-reading the Icelandic abstract. Finally, we thank Pierre Delmelle (Université catholique de Louvain) and two anonymous reviewers for their useful comments that materially improved the quality of the manuscript.

Data Availability

The data analysed in this paper are available to download from a data repository located at https://doi.org/10.7488/ds/3452 [Morison and Streeter 2022]. Supplementary Material is available alongside the online version of this article.

Copyright notice

References

Ágústsdóttir, A. M. (2015). "Ecosystem approach for natural hazard mitigation of volcanic tephra in Iceland: building resilience and sustainability". *Natural Hazards* 78(3), pages 1669–1691. DOI: 10.1007/s11069-015-1795-6.

Alfano, F., C. Bonadonna, S. Watt, C. Connor, A. Volentik, and D. M. Pyle (2016). "Reconstruction of total grain size distribution of the climactic phase of a long-lasting eruption: the example of the 2008–2013 Chaitén eruption". *Bulletin of Volcanology* 78(7). DOI: 10.1007/s00445-016-1040-5.

Andronico, D., S. Scollo, A. Cristaldi, and M. D. Lo Castro (2014). "Representivity of incompletely sampled fall deposits in estimating eruption source parameters: a test using the 12–13 January 2011 lava fountain deposit from Mt. Etna volcano, Italy". *Bulletin of Volcanology* 76(10). DOI: 10.1007/s00445-014-0861-3.

Arnalds, O., P. Dagsson-Waldhauserova, and H. Olafsson (2016). "The Icelandic volcanic aeolian environment: Processes and impacts — A review". *Aeolian Research* 20, pages 176–195. DOI: 10.1016/j.aeolia.2016.01.004.

Arnalds, O., E. F. Thorarinsdottir, J. Thorsson, P. D. Waldhauserova, and A. M. Agustsdottir (2013). "An extreme wind erosion event of the fresh Eyjafjallajökull 2010 volcanic ash". *Scientific Reports* 3(1). DOI: 10.1038/srep01257.

Ayris, P. M. and P. Delmelle (2012). "The immediate environmental effects of tephra emission". *Bulletin of Volcanology* 74(9), pages 1905–1936. DOI: 10.1007/s00445-012-0654-5.

Bagheri, G. and C. Bonadonna (2016). "Aerodynamics of Volcanic Particles". *Volcanic Ash*, pages 39–52. DOI: 10.1016/b978-0-08-100405-0.00005-7.

Barsotti, S., D. I. Di Rienzo, T. Thordarson, B. B. Björnsson, and S. Karlsdóttir (2018). "Assessing Impact to Infrastructures Due to Tephra Fallout From Öræfajökull Volcano (Iceland) by Using a Scenario-Based Approach and a Numerical Model". *Frontiers in Earth Science* 6. DOI: 10.3389/feart.2018.00196.

Beckett, F., A. Kylling, G. Sigurðardóttir, S. von Löwis, and C. Witham (2017). "Quantifying the mass loading of particles in an ash cloud remobilized from tephra deposits on Iceland". *Atmospheric Chemistry and Physics* 17(7), pages 4401–4418. DOI: 10.5194/acp-17-4401-2017.

Bjornstad, O. N. and J. Cai (2020). *ncf: spatial covariance functions. R package version 1.2-9*. https://CRAN.R-project.org/package=ncf.

Blockley, S. P. ., S. D. F. Pyne-O'Donnell, J. J. Lowe, I. P. Matthews, A. Stone, A. M. Pollard, C. S. M. Turney, and E. G. Molyneux (2005). "A new and less destructive laboratory procedure for the physical separation of distal glass tephra shards from sediments". *Quaternary Science Reviews* 24(16–17), pages 1952–1960. DOI: 10.1016/j.quascirev.2004.12.008.

Blong, R., N. Enright, and P. Grasso (2017). "Preservation of thin tephra". *Journal of Applied Volcanology* 6(1), pages 1–15. DOI: 10.1186/s13617-017-0059-4.

Blott, S. J., D. J. Croft, K. Pye, S. E. Saye, and H. E. Wilson (2004). "Particle size analysis by laser diffraction". *Geological Society, London, Special Publications* 232(1), pages 63–73. DOI: 10.1144/gsl.sp.2004.232.01.08.

Blott, S. J. and K. Pye (2001). "GRADISTAT: a grain size distribution and statistics package for the analysis of unconsolidated sediments". *Earth Surface Processes and Landforms* 26(11), pages 1237–1248. DOI: 10.1002/esp.261.

Bonadonna, C., R. Cioni, M. Pistolesi, M. Elissondo, and V. Baumann (2015). "Sedimentation of long-lasting wind-affected volcanic plumes: the example of the 2011 rhyolitic Cordón Caulle eruption, Chile". *Bulletin of Volcanology* 77(2). DOI: 10.1007/s00445-015-0900-8.

Bonadonna, C., R. Genco, M. Gouhier, M. Pistolesi, R. Cioni, F. Alfano, A. Hoskuldsson, and M. Ripepe (2011). "Tephra sedimentation during the 2010 Eyjafjallajökull eruption (Iceland) from deposit, radar, and satellite observations". *Journal of Geophysical Research* 116(B12). DOI: 10.1029/2011jb008462.

Bonadonna, C. and B. F. Houghton (2005). "Total grain-size distribution and volume of tephra-fall deposits". *Bulletin of Volcanology* 67(5), pages 441–456. DOI: 10.1007/s00445-004-0386-2.

Breshears, D. D., J. J. Whicker, C. B. Zou, J. P. Field, and C. D. Allen (2009). "A conceptual framework for dryland aeolian sediment transport along the grassland–forest continuum: Effects of woody plant canopy cover and disturbance". *Geomorphology* 105(1–2), pages 28–38. DOI: 10.1016/j.geomorph.2007.12.018.

Buckland, H. M., K. V. Cashman, S. L. Engwell, and A. C. Rust (2020). "Sources of uncertainty in the Mazama isopachs and the implications for interpreting distal tephra deposits from large magnitude eruptions". *Bulletin of Volcanology* 82(3). DOI: 10.1007/s00445-020-1362-1.

Buckland, H. M., J. Saxby, M. Roche, P. Meredith, A. C. Rust, K. V. Cashman, and S. L. Engwell (2021). "Measuring the size of non-spherical particles and the implications for grain size analysis in volcanology". *Journal of Volcanology and Geothermal Research* 415, page 107257. DOI: 10.1016/j.jvolgeores.2021.107257.

Cabré, J., M. Aulinas, M. Rejas, and J. L. Fernandez-Turiel (2016). "Volcanic ash leaching as a means of tracing the environmental impact of the 2011 Grímsvötn eruption, Iceland". *Environmental Science and Pollution Research* 23(14), pages 14338–14353. DOI: 10.1007/s11356-016-6559-7.

Carey, R. J., B. F. Houghton, and T. Thordarson (2010). "Tephra dispersal and eruption dynamics of wet and dry phases of the 1875 eruption of Askja Volcano, Iceland". *Bulletin of Volcanology* 72(3), pages 259–278. DOI: 10.1007/s00445-009-0317-3.

Carey, S. N. and H. Sigurdsson (1982). "Influence of particle aggregation on deposition of distal tephra from the May 18, 1980, eruption of Mount St. Helens volcano". *Journal of Geophysical Research: Solid Earth* 87(B8), pages 7061–7072. DOI: 10.1029/jb087ib08p07061.

Cashman, K. V. and A. C. Rust (2019). "Far-travelled ash in past and future eruptions: combining tephrochronology with volcanic studies". *Journal of Quaternary Science* 35(1–2), pages 11–22. DOI: 10.1002/jqs.3159.

Costa, A., L. Pioli, and C. Bonadonna (2016). "Assessing tephra total grain-size distribution: Insights from field data analysis". *Earth and Planetary Science Letters* 443, pages 90–107. DOI: 10.1016/j.epsl.2016.02.040.

Cutler, N. A., R. M. Bailey, K. T. Hickson, R. T. Streeter, and A. J. Dugmore (2016a). "Vegetation structure influences the retention of airfall tephra in a sub-Arctic landscape". *Progress in Physical Geography: Earth and Environment* 40(5), pages 661–675. DOI: 10.1177/0309133316650618.

Cutler, N. A., O. M. Shears, R. T. Streeter, and A. J. Dugmore (2016b). "Impact of small-scale vegetation structure on tephra layer preservation". *Scientific Reports* 6(1). DOI: 10.1038/srep37260.

Cutler, N. A., R. T. Streeter, A. J. Dugmore, and E. R. Sear (2021). "How do the grain size characteristics of a tephra deposit change over time?" *Bulletin of Volcanology* 83(7). DOI: 10.1007/s00445-021-01469-w.

Cutler, N. A., R. T. Streeter, S. L. Engwell, M. S. Bolton, B. J. L. Jensen, and A. J. Dugmore (2020). "How does tephra deposit thickness change over time? A calibration exercise based on the 1980 Mount St Helens tephra deposit". *Journal of Volcanology and Geothermal Research* 399, page 106883. DOI: 10.1016/j.jvolgeores.2020.106883.

Cutler, N. A., R. T. Streeter, J. Marple, L. R. Shotter, J. S. Yeoh, and A. J. Dugmore (2018). "Tephra transformations: variable preservation of tephra layers from two well-studied eruptions". *Bulletin of Volcanology* 80(11). DOI: 10.1007/s00445-018-1251-z.

Del Bello, E., J. Taddeucci, J. P. Merrison, S. Alois, J. J. Iversen, and P. Scarlato (2018). "Experimental simulations of volcanic ash resuspension by wind under the effects of atmospheric humidity". *Scientific Reports* 8(1). DOI: 10.1038/s41598-018-32807-2.

Del Bello, E., J. Taddeucci, J. Merrison, K. Rasmussen, D. Andronico, T. Ricci, P. Scarlato, and J. Iversen (2021). "Field-based measurements of volcanic ash resuspension by wind". *Earth and Planetary Science Letters* 554, page 116684. DOI: 10.1016/j.epsl.2020.116684.

Domínguez, L., C. Bonadonna, P. Forte, P. A. Jarvis, R. Cioni, L. Mingari, D. Bran, and J. E. Panebianco (2020). "Aeolian Remobilisation of the 2011-Cordón Caulle Tephra-Fallout Deposit: Example of an Important Process in the Life Cycle of Volcanic Ash". *Frontiers in Earth Science* 7. DOI: 10.3389/feart.2019.00343.

Dugmore, A. J. and A. J. Newton (2012). "Isochrons and beyond: maximising the use of tephrochronology in geomorphology". *Jökull* 62, pages 39–52.

Dugmore, A. J., A. J. Newton, G. Larsen, and G. T. Cook (2000). "Tephrochronology, Environmental Change and the Norse Settlement of Iceland". *Environmental Archaeology* 5(1), pages 21–34. DOI: 10.1179/env.2000.5.1.21.

Dugmore, A. J., A. J. Newton, K. T. Smith, and K.-A. Mairs (2013). "Tephrochronology and the late Holocene volcanic and flood history of Eyjafjallajökull, Iceland". *Journal of Quaternary Science* 28(3), pages 237–247. DOI: 10.1002/jqs.2608.

Dugmore, A. J., R. Streeter, and N. A. Cutler (2018). "The role of vegetation cover and slope angle in tephra layer preservation and implications for Quaternary tephrostratigraphy". *Palaeogeography, Palaeoclimatology, Palaeoecology* 489, pages 105–116. DOI: 10.1016/j.palaeo.2017.10.002.

Dugmore, A. J., P. I. J. Thompson, R. T. Streeter, N. A. Cutler, A. J. Newton, and M. P. Kirkbride (2019). "The interpretative value of transformed tephra sequences". *Journal of Quaternary Science* 35(1–2), pages 23–38. DOI: 10.1002/jqs.3174.

Durant, A. J., W. I. Rose, A. M. Sarna-Wojcicki, S. Carey, and A. C. M. Volentik (2009). "Hydrometeor-enhanced tephra sedimentation: Constraints from the 18 May 1980 eruption of Mount St. Helens". *Journal of Geophysical Research* 114(B3). DOI: 10.1029/2008jb005756.

Engwell, S., R. Sparks, and W. Aspinall (2013). "Quantifying uncertainties in the measurement of tephra fall thickness". *Journal of Applied Volcanology* 2(1). DOI: 10.1186/2191-5040-2-5.

Eshel, G., G. J. Levy, U. Mingelgrin, and M. J. Singer (2004). "Critical Evaluation of the Use of Laser Diffraction for Particle-Size Distribution Analysis". *Soil Science Society of America Journal* 68(3), pages 736–743. DOI: 10.2136/sssaj2004.7360.

Essery, R. and J. Pomeroy (2004). "Vegetation and Topographic Control of Wind-Blown Snow Distributions in Distributed and Aggregated Simulations for an Arctic Tundra Basin". *Journal of Hydrometeorology* 5(5), pages 735–744. DOI: 10.1175/1525-7541(2004)005<0735:vatcow>2.0.co;2.

Etyemezian, V., J. A. Gillies, L. G. Mastin, A. Crawford, R. Hasson, A. R. Van Eaton, and G. Nikolich (2019). "Laboratory Experiments of Volcanic Ash Resuspension by Wind". *Journal of Geophysical Research: Atmospheres* 124(16), pages 9534–9560. DOI: 10.1029/2018jd030076.

Eychenne, J., J.-L. Le Pennec, L. Troncoso, M. Gouhier, and J.-M. Nedelec (2011). "Causes and consequences of bimodal grain-size distribution of tephra fall deposited during the August 2006 Tungurahua eruption (Ecuador)". *Bulletin of Volcanology* 74(1), pages 187–205. DOI: 10.1007/s00445-011-0517-5.

Forte, P., L. Domínguez, C. Bonadonna, C. E. Gregg, D. Bran, D. Bird, and J. M. Castro (2018). "Ash resuspension related to the 2011–2012 Cordón Caulle eruption, Chile, in a rural community of Patagonia, Argentina". *Journal of Volcanology and Geothermal Research* 350, pages 18–32. DOI: 10.1016/j.jvolgeores.2017.11.021.

Gatti, E., M. Saidin, K. Talib, N. Rashidi, P. Gibbard, and C. Oppenheimer (2013). "Depositional processes of reworked tephra from the Late Pleistocene Youngest Toba Tuff deposits in the Lenggong Valley, Malaysia". *Quaternary Research* 79(2), pages 228–241. DOI: 10.1016/j.yqres.2012.11.006.

Gee, G. W. and J. W. Bauder (1980). "Particle Size Analysis by Hydrometer: A Simplified Method for Routine Textural Analysis and a Sensitivity Test of Measurement Parameters". *Soil Science Society of America Journal* 43(5), pages 1004–1007. DOI: 10.2136/sssaj1979.03615995004300050038x.

– (1986). "Particle-size analysis". *Methods of soil analysis. Part 1. Physical and mineralogical methods.* Edited by A. Klute. Volume 5. Madison, WI.: Soil Science Society of America, pages 383–411. ISBN: 9780891188643. DOI: 10.2136/sssabookser5.1.2ed. 2nd edition.

Gisladottir, F. O., O. Arnalds, and G. Gisladottir (2005). "The effect of landscape and retreating glaciers on wind erosion in South Iceland". *Land Degradation & Development* 16(2), pages 177–187. DOI: 10.1002/ldr.645.

Gislason, S. R., T. Hassenkam, S. Nedel, N. Bovet, E. S. Eiriksdottir, H. A. Alfredsson, C. P. Hem, Z. I. Balogh, K. Dideriksen, N. Oskarsson, B. Sigfusson, G. Larsen, and S. L. S. Stipp (2011). "Characterization of Eyjafjallajökull volcanic ash particles and a protocol for rapid risk assessment". *Proceedings of the National Academy of Sciences* 108(18), pages 7307–7312. DOI: 10.1073/pnas.1015053108.

Gudmundsson, M. T., T. Thordarson, Á. Höskuldsson, G. Larsen, H. Björnsson, F. J. Prata, B. Oddsson, E. Magnússon, T. Högnadóttir, G. N. Petersen, C. L. Hayward, J. A. Stevenson, and I. Jónsdóttir (2012a). "Ash generation and distribution from the April-May 2010 eruption of Eyjafjallajökull, Iceland". *Scientific Reports* 2(1). DOI: 10.1038/srep00572.

Gudmundsson, M. T., Á. Höskuldsson, G. Larsen, T. Thordarson, B. A. Oladottir, B. Oddsson, J. Gudnason, T. Högnadottir, J. A. Stevenson, B. F. Houghton, D. McGarvie, and G. M. Sigurdardottir (2012b). "The May 2011 eruption of Grímsvötn". *EGU General Assembly Conference Abstracts*, page 12119.

Hall, K. and C. Thorn (2011). "The historical legacy of spatial scales in freeze–thaw weathering: Misrepresentation and resulting misdirection". *Geomorphology* 130(1–2), pages 83–90. DOI: 10.1016/j.geomorph.2010.10.003.

Hiemstra, C. A., G. E. Liston, and W. A. Reiners (2002). "Snow Redistribution by Wind and Interactions with Vegetation at Upper Treeline in the Medicine Bow Mountains, Wyoming, U.S.A." *Arctic, Antarctic, and Alpine Research* 34(3), pages 262–273. DOI: 10.1080/15230430.2002.12003493.

– (2006). "Observing, modelling, and validating snow redistribution by wind in a Wyoming upper treeline landscape". *Ecological Modelling* 197(1–2), pages 35–51. DOI: 10.1016/j.ecolmodel.2006.03.005.

Horwell, C., P. Baxter, S. Hillman, J. Calkins, D. Damby, P. Delmelle, K. Donaldson, C. Dunster, B. Fubini, F. Kelly, J. Le Blond, K. Livi, F. Murphy, C. Nattrass, S. Sweeney, T. Tetley, T. Thordarson, and M. Tomatis (2013). "Physicochemical and toxicological profiling of ash from the 2010 and 2011 eruptions of Eyjafjallajökull and Grímsvötn volcanoes, Iceland using a rapid respiratory hazard assessment protocol". *Environmental Research* 127, pages 63–73. DOI: 10.1016/j.envres.2013.08.011.

Hotes, S., P. Poschlod, H. Takahashi, A. P. Grootjans, and E. Adema (2004). "Effects of tephra deposition on mire vegetation: a field experiment in Hokkaido, Japan". *Journal of Ecology*, pages 624–634.

Inman, D. L. (1952). "Measures for Describing the Size Distribution of Sediments". *SEPM Journal of Sedimentary Research* 22(3), pages 125–145. DOI: 10.1306/d42694db-2b26-11d7-8648000102c1865d.

Janebo, M. H., B. F. Houghton, T. Thordarson, C. Bonadonna, and R. J. Carey (2018). "Total grain-size distribution of four subplinian–Plinian tephras from Hekla volcano, Iceland: Implications for sedimentation dynamics and eruption source parameters". *Journal of Volcanology and Geothermal Research* 357, pages 25–38. DOI: 10.1016/j.jvolgeores.2018.04.001.

Larsen, G. and J. Eiríksson (2008). "Late Quaternary terrestrial tephrochronology of Iceland—frequency of explosive eruptions, type and volume of tephra deposits". *Journal of Quaternary Science* 23(2), pages 109–120. DOI: 10.1002/jqs.1129.

Liu, E. J., K. V. Cashman, F. M. Beckett, C. S. Witham, S. J. Leadbetter, M. C. Hort, and S. Guðmundsson (2014). "Ash mists and brown snow: Remobilization of volcanic ash from recent Icelandic eruptions". *Journal of Geophysical Research: Atmospheres* 119(15), pages 9463–9480. DOI: 10.1002/2014jd021598.

Lowe, D. J. (2011). "Tephrochronology and its application: A review". *Quaternary Geochronology* 6(2), pages 107–153. DOI: 10.1016/j.quageo.2010.08.003.

Lowe, D. J. and J. B. Hunt (2001). "A summary of terminology used in tephra-related studies". *Tephras: Chronology, Archaeology.* Volume Les Dossiers de l'Archaeo-logis 1. Centre de recherches archéologiques départemental, pages 17–22.

Morison, C. A. G. (2020). "Variable Preservation of Volcanic Ash from the Eyjafjallajökull (2010) and Grímsvötn (2011) Eruptions". Master of Science by Research thesis. University of St Andrews, UK.

Morison, C. A. G. and R. T. Streeter (2022). *The influence of vegetation cover on the grain-size distributions and thicknesses of two Icelandic tephra layers, 2019.* https://doi.org/10.7488/ds/3452. [dataset].

Mueller, S. B., U. Kueppers, J. Ametsbichler, C. Cimarelli, J. P. Merrison, M. Poret, F. B. Wadsworth, and D. B. Dingwell (2017). "Stability of volcanic ash aggregates and break-up processes". *Scientific Reports* 7(1). DOI: 10.1038/s41598-017-07927-w.

National Land Survey of Iceland (2012). *Landscape*. URL: http://kortasja.lmi.is/en/ (visited on 10/24/2019).

Newhall, C. G. and S. Self (1982). "The volcanic explosivity index (VEI) an estimate of explosive magnitude for historical volcanism". *Journal of Geophysical Research* 87(C2), page 1231. DOI: 10.1029/jc087ic02p01231.

Óladóttir, B. A., G. Larsen, and O. Sigmarsson (2011). "Holocene volcanic activity at Grímsvötn, Bárdarbunga and Kverkfjöll subglacial centres beneath Vatnajökull, Iceland". *Bulletin of Volcanology* 73(9), pages 1187–1208. DOI: 10.1007/s00445-011-0461-4.

Olsson, J., S. Stipp, K. Dalby, and S. Gislason (2013). "Rapid release of metal salts and nutrients from the 2011 Grímsvötn, Iceland volcanic ash". *Geochimica et Cosmochimica Acta* 123, pages 134–149. DOI: 10.1016/j.gca.2013.09.009.

Panebianco, J. E., M. J. Mendez, D. E. Buschiazzo, D. Bran, and J. J. Gaitán (2017). "Dynamics of volcanic ash remobilisation by wind through the Patagonian steppe after the eruption of Cordón Caulle, 2011". *Scientific Reports* 7(1). DOI: 10.1038/srep45529.

Paradis, E. and K. Schliep (2019). "ape 5.0: an environment for modern phylogenetics and evolutionary analyses in R". *Bioinformatics* 35(3). Edited by R. Schwartz, pages 526–528. DOI: 10.1093/bioinformatics/bty633.

Paredes-Mariño, J., P. Forte, S. Alois, K. L. Chan, V. Cigala, S. B. Mueller, M. Poret, A. Spanu, I. Tomašek, P.-Y. Tournigand, D. Perugini, and U. Kueppers (2022). "The lifecycle of volcanic ash: advances and ongoing challenges". *Bulletin of Volcanology* 84(5). DOI: 10.1007/s00445-022-01557-5.

Pioli, L., C. Bonadonna, and M. Pistolesi (2019). "Reliability of Total Grain-Size Distribution of Tephra Deposits". *Scientific Reports* 9(1). DOI: 10.1038/s41598-019-46125-8.

Poret, M., M. Di Donato, A. Costa, R. Sulpizio, D. Mele, and F. Lucchi (2020). "Characterizing magma fragmentation and its relationship with eruptive styles of Somma-Vesuvius volcano (Naples, Italy)". *Journal of Volcanology and Geothermal Research* 393, page 106683. DOI: 10.1016/j.jvolgeores.2019.106683.

Prata, F., M. Woodhouse, H. E. Huppert, A. Prata, T. Thordarson, and S. Carn (2017). "Atmospheric processes affecting the separation of volcanic ash and SO_2; in volcanic eruptions: inferences from the May 2011 Grímsvötn eruption". *Atmospheric Chemistry and Physics* 17(17), pages 10709–10732. DOI: 10.5194/acp-17-10709-2017.

Sarna-Wojcicki, A. M., S. Shipley, R. B. Waitt, D. Dzurisin, and S. Wood (1981). "Areal distribution, thickness, mass, volume and grain-size of air-fall ash from the six major eruptions in 1980". *The 1980 eruptions of Mount St. Helens, Washington*. Edited by P. W. Lipman and D. R. Mullineaux. U.S. Geological Survey, pages 577–600. DOI: 10.3133/pp1250. Professional Paper 1250.

Shao, Y. and H. Lu (2000). "A simple expression for wind erosion threshold friction velocity". *Journal of Geophysical Research: Atmospheres* 105(D17), pages 22437–22443. DOI: 10.1029/2000jd900304.

Sohn, C. and Y. K. Sohn (2019). "Distinguishing between primary and secondary volcaniclastic deposits". *Scientific Reports* 9(1). DOI: 10.1038/s41598-019-48933-4.

Streeter, R. and A. J. Dugmore (2013). "Anticipating land surface change". *Proceedings of the National Academy of Sciences* 110(15), pages 5779–5784. DOI: 10.1073/pnas.1220161110.

Streeter, R., A. J. Dugmore, I. T. Lawson, E. Erlendsson, and K. J. Edwards (2015). "The onset of the palaeoanthropocene in Iceland: Changes in complex natural systems". *The Holocene* 25(10), pages 1662–1675. DOI: 10.1177/0959683615594468.

Taddeucci, J., P. Scarlato, D. Andronico, A. Cristaldi, R. Büttner, B. Zimanowski, and U. Küppers (2007). "Advances in the study of volcanic ash". *Eos, Transactions American Geophysical Union* 88(24), pages 253–256. DOI: 10.1029/2007eo240001.

Taddeucci, J., P. Scarlato, C. Montanaro, C. Cimarelli, E. Del Bello, C. Freda, D. Andronico, M. T. Gudmundsson, and D. B. Dingwell (2011). "Aggregation-dominated ash settling from the Eyjafjallajökull volcanic cloud illuminated by field and laboratory high-speed imaging". *Geology* 39(9), pages 891–894. DOI: 10.1130/g32016.1.

Tarasenko, I., C. L. Bielders, A. Guevara, and P. Delmelle (2019). "Surface crusting of volcanic ash deposits under simulated rainfall". *Bulletin of Volcanology* 81(5). DOI: 10.1007/s00445-019-1289-6.

Thompson, P. I. J., A. J. Dugmore, A. J. Newton, R. T. Streeter, and N. A. Cutler (2021). "Variations in tephra stratigraphy created by small-scale surface features in sub-polar landscapes". *Boreas* 51(2), pages 317–331. DOI: 10.1111/bor.12557.

Thorarinsdottir, E. F. and O. Arnalds (2012). "Wind erosion of volcanic materials in the Hekla area, South Iceland". *Aeolian Research* 4, pages 39–50. DOI: 10.1016/j.aeolia.2011.12.006.

Thorarinsson, S. (1954). "The eruption of Hekla, 1947-1948, Part II 3. The tephra-fall from Hekla on March 29 th, 1947". *Visindafelag Islendinga* 68.

– (1958). "The Öræfajökull eruption of 1362". *Acta Naturalia Islandica* 2(2), pages 1–99.

Thordarson, T. and Á. Höskuldsson (2008). "Postglacial volcanism in Iceland". *Jökull* 58(198), e228.

– (2020). *Iceland*. Volume Classic Geology in Europe 3. Edinburgh: Dunedin Academic Press Ltd. ISBN: 9781780460925.

Thordarson, T. and G. Larsen (2007). "Volcanism in Iceland in historical time: Volcano types, eruption styles and eruptive history". *Journal of Geodynamics* 43(1), pages 118–152. DOI: 10.1016/j.jog.2006.09.005.

Thorsteinsson, T., T. Jóhannsson, A. Stohl, and N. I. Kristiansen (2012). "High levels of particulate matter in Iceland due to direct ash emissions by the Eyjafjallajökull eruption and resuspension of deposited ash". *Journal of Geophysical Research: Solid Earth* 117(B9). DOI: 10.1029/2011jb008756.

Tsunematsu, K. and C. Bonadonna (2015). "Grain-size features of two large eruptions from Cotopaxi volcano (Ecuador) and implications for the calculation of the total grain-size distribution". *Bulletin of Volcanology* 77(7). DOI: 10.1007/s00445-015-0949-4.

Veðurstofa Íslands (2012). *Climatological data for Samsstaðir and Kirkjubæjarklaustur*. URL: https://en.vedur.is/climatology/data/ (visited on 01/18/2021).

Wentworth, C. K. (1922). "A scale of grade and class terms for clastic sediments". *The Journal of Geology* 30(5), pages 377–392.

White, J. and B. Houghton (2006). "Primary volcaniclastic rocks". *Geology* 34(8), page 677. DOI: 10.1130/g22346.1.

Wilson, T. M., J. W. Cole, C. Stewart, S. J. Cronin, and D. M. Johnston (2011). "Ash storms: impacts of wind-remobilised volcanic ash on rural communities and agriculture following the 1991 Hudson eruption, southern Patagonia, Chile". *Bulletin of Volcanology* 73(3), pages 223–239. DOI: 10.1007/s00445-010-0396-1.

Wolfe, S. A. and W. G. Nickling (1993). "The protective role of sparse vegetation in wind erosion". *Progress in Physical Geography: Earth and Environment* 17(1), pages 50–68. DOI: 10.1177/030913339301700104.